Genome wide association analysis of resistance to scald in an adapted multiparent winter malting barley population

J.M. Kolkman[1,2,*], S.S. Sepp[1], K. Kunze[1], G.C. Bergstrom[2], and M.E. Sorrells[1]

Affiliations

[1] Plant Breeding and Genetics Section, School of Integrative Plant Science, Cornell University, Ithaca, NY, USA
[2] Plant Pathology and Plant-Microbe Biology Section, School of Integrative Plant Science, Cornell University, Ithaca, NY, USA
*Corresponding Author: Judith M. Kolkman (jmk87@cornell.edu)

Core Ideas

- Resistance to scald in a large multiparent population was derived from a major resistance gene (*Rrs1*) and several smaller effect QTLs
- *Rrs1* resistance was derived from 'Lightning' and is located within a large linkage block on Chromosome 3H
- Fewer days to heading and taller plants were correlated with less disease in a large multiparent winter malting barley population in NY state
- A QTL for resistance to scald co-localized on chromosome 2H with winter survival, heading date, and plant height
- FarmCPU was an optimal model for association analysis for resistance to scald in the large unbalanced diallel population.

ABSTRACT

Scald, caused by the fungus *Rhynchosporium graminicola* Heinsen 1897, is a major foliar disease in winter malting barley (*Hordeum vulgare* L). Resistance to scald in winter malting barley is controlled by major and minor resistance genes. We used a large population of lines derived from biparental crosses among five winter malting barley parents to analyze resistance to scald and associated agronomic traits. Increased winter survival and later heading dates were negatively correlated with increased resistance, whereas increased height was positively correlated with resistance. A genome-wide association study (GWAS) for resistance to scald was analyzed with multiple models, using 15,463 SNPs. The similarities and differences between the models were identified in SNP trait associations and phenotypic effect sizes. SNP associations identified a large region on chromosome 3H across models. FarmCPU identified additional associations on chromosomes 2H, 3H, and 4H. Linkage disequilibrium on chromosome 3H and GWAS for resistance to scald using the *Rrs1*-linked marker, HVS3, as a covariate confirmed *Rrs1* was segregating in this population. GWAS for winter survival, heading date and plant height identified associations across the genome, with chromosome 2H showing SNP-trait colocalizations between resistance to scald, winter survival, heading date and plant height. Breeding for durable resistance to scald in winter malting barley can include pyramiding major resistance loci, such as *Rrs1*, as well as QTL for disease resistance and agronomic traits.

PLAIN LANGUAGE SUMMARY

Genetic architecture of resistance to scald in winter malting barley

Scald is an important foliar pathogen in winter malting barley, affecting both grain yield and quality. While resistance to scald is controlled by major and minor resistance genes, agronomic traits are also known to limit the spread of scald in barley. We determined the genetic architecture using a large multiparent population of winter malting barley. The FarmCPU genome-wide association model proved optimal for defining the resistance genes, with the major resistance gene, *Rrs1*, conferring 27% of the variation in this population. Fewer days to heading and taller plants contributed to plant avoidance of scald. Reduced canopy coverage in plants with low winter survival led to less scald severity. A region of the genome contributing a minor resistance effect was co-localized with a region for plant height, heading date and winter survival.

Abbreviations

BLINK, Bayesian-information and linkage-disequilibrium iteratively nested keyway
DLA, diseased leaf area
FarmCPU, fixed and random model circulating probability unification
GAPIT, genome association and prediction integrated tool
GWAS, genome wide association study
HT, height
LD, linkage disequilibrium
LRR-RLK, leucine-rich repeat receptor-like proteins
MAF, minor allele frequency
MAGIC, multiple advanced generation inbred cross
MTA, marker trait association
MLM, mixed linear model
MLMM, multiple loci mixed linear model
PCA, principal components analysis
SNP, single nucleotide polymorphism
QTL, quantitative trait loci
PEI, pectin esterase inhibitor
QQ, quantile-quantile
Reml, restricted maximum likelihood model
SCAR, sequenced characterized amplified region
PVE, phenotypic variation explained
WS, winter survival

1 INTRODUCTION

Barley, *Hordeum vulgare* L., is a globally important crop used for livestock feed, human food, and for malt used in brewed and distilled beverages. The increased demand for malting barley by the craft brewing industry has led to increased malting barley production in non-traditional barley growing regions (Shrestha & Lindsey, 2019). The adoption of malting barley in the Northeast US has been

fostered by development of improved management recommendations for barley grown in higher rainfall and more humid conditions than in traditional barley growing regions (Shrestha & Lindsey, 2019; Siller et al., 2021). Winter barley offers consistently higher yield and often higher quality than spring barley and often avoids unfavorable spring planting conditions and summer droughts. Along with agronomic management differences, a shift from spring to winter malting barley alters the disease exposure profile, resulting in an environment conducive to the proliferation of scald. Barley scald is a foliar fungal pathogen, that flourishes in the cooler climates reaching up to 77% diseased leaf area of upper canopy during early grain filling stages in susceptible cultivars grown in New York (Kolkman et al., 2025a). Scald can cause both a reduction in quality (Avrova & Knogge, 2012), and yield losses ranging from 10 to 45% (Shipton et al., 1974), and up to 65% in severe epidemics (Beigi et al., 2013).

Scald in barley is caused by *Rhynchosporium graminicola* Heinsen 1897 (Crous et al., 2021; formerly known *as R. commune*; Zaffarano, et al., 2011) a hemibiotrophic foliar fungal pathogen that thrives in cooler temperatures (Zaffarano et al., 2008). Originally identified in 1897 (Frank, 1987), *R. graminicola* was renamed as *R. secalis* (Oudem.) J.J. Davis in 1919 (Davis, 1919), renamed again in 2008 as *R. commune* indicate host speciation specific to *Hordeum* species (Zaffarano et al., 2008, 2011). *Rhynchosporium graminicola* is proposed to have originated in the cool climates of Scandinavia approximately 2500 years ago as a host jump from an unknown grass species (Brunner et al., 2007). *R. graminicola* spreads through previously infected barley debris and/or infected seed (Ababa et al., 2023). Conidia land on leaf surfaces and produce a germ tube along the intercellular grooves that produces an appressorium that penetrates through the cuticle, all within the first 24 hours of exposure (Linsell et al., 2011). Hyphae grow below the cuticle, above the anticlinal walls and between the epidermal cells, between the pectin layer and outer cell wall, disrupting the pectic layer and cuticle for pectin degradation (Ayesu-Offei & Clarke, 1970; Ryan & Grivell, 1974; Lehnackers & Knogge, 1990; Linsell et al., 2011). The cuticle and epidermal layers separate with the production of a packed hyphal mat, forming a subcuticular stroma, inducing a water-soaked lesion, all within approximately 4 to 8 days (Ayesu-Offei & Clarke, 1970; Linsell et al., 2011). Mesophyll collapse follows approximately 7 to 14 days post inoculation, creating a straw-colored necrotic lesion surrounded by dark brown borders at which point hyphal growth increased, likely due to the release of nutrients from the collapsed mesophyll cells (Ayesu-Offei & Clarke, 1970; Lehnackers & Knogge, 1990; Linsell et al., 2011). Conidia are produced from subcuticular and/or substomatal stroma, which protrude through the cuticle along the leaf surface.

Resistance to scald in barley has been attributed to both major resistance genes and quantitative trait loci (QTLs; as reviewed by Zhang et al., 2020). In total, 11 major resistance genes have been described (as compiled by Noe et al., 2025) with major resistance genes located on all chromosomes except chromosome 5H. Several of the *Rrs* genes are comprised of multiple alleles and/or loci, such as the *Rrs1* gene complex located on chromosome 3H that includes the previously described alleles *Rh*, *Rh1*, *Rh3* *Rh4* and *Rh7* (Bjørnstad et al., 2002). While no causal gene underlying the *Rrs* genes has been determined, several *Rrs* genes have been fine-mapped. The *Rrs1* gene region has been delimited to a region of 0.8 Mb with 10 candidate genes using the Morex genome sequence. The *Rrs1* gene is not, however, present in the Morex genome, and is hypothesized to be presence-absence and/or a gene duplication variant. There are several candidates that are plausible in this genomic region that is reticent to recombination, due to its centromeric location, including a protein kinase (Looseley et al., 2020). The *Rrs2* resistance gene is proposed to be in a cluster of pectin esterase inhibitor (PEI) genes, either as a unique gene, a combination of PEI genes and/or other unidentified gene(s) (Marzin et al., 2016). The

127 *Rrs13* resistance gene, fine-mapped within a 0.58 to 1.2 Mbp region, codes for two to seven tandemly
128 repeated leucine-rich repeat receptor-like proteins (LRR-RLP) and a lectin receptor-like kinase (Eckstein
129 et al., 2024). More recently, the *Rrs18* gene has been identified upstream of *Rrs13* (Coulter et al., 2019).
130 Fine-mapping and RNA expression analysis identified four candidate genes with the most likely candidate
131 gene a serine/threonine protein kinase. As well as these four genes, a stable QTL for adult plant
132 resistance to scald, QSc.VR4, was fine-mapped to a 0.38 Mbp region that included an LRR-RLK multi-gene
133 family, and a germin-like protein multigene family (Wang et al., 2020).

134 Numerous genome-wide association studies (GWAS) have been utilized to identify and characterize
135 resistance to scald in barley. Association studies have relied on a variety of populations, including
136 diversity panels (Looseley et al., 2018; Hiddar et al., 2023; Kunze et al., 2024; Noe et al., 2025), a multiple
137 advanced generation inbred cross (MAGIC) population (Hautsalo et al., 2021), the HEB25 nested
138 association mapping population (Büttner et al., 2020), and a variety of populations that included diverse
139 germplasm, including landraces, wild species and breeding lines (Looseley et al., 2018, 2020; Clare et al.,
140 2023; Ababa et al., 2024; Ijaz et al., 2024). Many trials utilize greenhouse trials to ascertain seedling
141 resistance (major gene resistance), using one or more isolates to characterize resistance to specific
142 isolates. Several studies relied on (natural) field infection to identify adult plant resistance (Daba et al.,
143 2019; Looseley et al., 2020; Ijaz et al., 2024). All GWAS studies used spring barley, except for two studies
144 that used spring, winter and/or facultative barley lines (Looseley et al., 2020; Kunze et al., 2024). Adult
145 plant resistance in the field encompasses natural infection, and resistance comprised of major resistance
146 (*Rrs*) genes and/or QTL for resistance to scald. Adult plant resistance has been associated with genes
147 coding for plant growth traits, such as *sdw1*, the gibberellin 2-oxidase gene, *HvGA20ox2* (Xu et al., 2017),
148 implicated with plant height and susceptibility to scald (Looseley et al., 2018). Improving barley for
149 resistance to scald relies on agronomic practices as well as breeding for resistance. Due to the potential
150 for *R. graminicola* populations to overcome resistance (Mcdonald, 2015; Ababa et al., 2024),
151 understanding the facets of resistance is imperative in breeding for sustainable resistance.

152 Genome wide association studies are useful for the identification of marker-trait associations and
153 characterization of trait architecture across the genome. The premise of GWAS relies on maximizing
154 meiotic recombination events by utilizing populations consisting of a large diverse number of genotypes
155 in conjunction with high SNP marker density, and in many cases, using population structure and kinship
156 to minimize false positive results (Flint-Garcia et al., 2005; Yu et al., 2006). Several models of GWAS have
157 been developed that use different approaches to identify marker trait associations (Tibbs Cortes et al.,
158 2021). In contrast, breeding programs are targeted to regional adaptation and are generally limited to
159 elite material based on founders and the introgression of adapted material that may have originated
160 from diverse or pre-breeding efforts (Kelly et al., 1998). Large populations are created with the goal of
161 finding the transgressive segregants that move crop development and the release of novel cultivars
162 forward.

163 In this study we characterized resistance to scald in a large unbalanced diallel breeding population of
164 winter malting barley recombinant inbred lines and doubled haploids derived from biparental crosses
165 between five founder lines that are adapted to New York environments. We examined the correlation of
166 agronomic traits, such as winter survival, days to heading and plant height with resistance to scald as a
167 means of escape and/or avoidance mechanisms. Using GWAS, we characterized the genetic
168 architecture of resistance to scald in the multiparent population, and the co-localization of SNP
169 associations between resistance to scald and winter survival, heading date and plant height. We explore

a suite of GWAS models available in GAPIT version 3 (Wang & Zhang, 2021) to determine the appropriate GWAS model for the multiparent unbalanced diallel population, given the relatedness and limited meiotic recombinant events between lines within the germplasm.

2 MATERIALS AND METHODS

2.1 Germplasm and trait phenotyping

2.1.1 Plant germplasm

A large population of winter malting barley breeding lines was derived from an unbalanced diallel mating design using five malting barley cultivars, including 'Flavia', 'Lightning' (Hayes et al., 2021), 'KWS Scala', 'SY Tepee', and 'WintMalt' and the corresponding 10 cross combinations. F_1 plants were advanced to the F_5 stage through single seed descent and/or through creating doubled haploids resulting in 377 recombinant inbred lines and doubled haploid lines (Figure 1).

2.1.2 Field trials

The diallel population was planted in four field sites (environments) at the Cornell University Campus Area Farms in Tompkins County near Ithaca, New York and included the Snyder Farm and Helfer Farm field sites in 2022, and the McGowan Farm and Ketola Farm field sites in 2023. Trials were grown in an augmented design with a single replication in each environment and included the parental cultivars as well as check cultivars ('KWS Scala', 'Lightning' and 'Endeavor') within four blocks in both 2022 environments (Snyder Farm and Helfer Farm), and within eight and ten blocks in Ketola Farm and McGowan Farm field sites in 2023, respectively. Seeds were planted in plots with 1.2 m width, 3.0 m plot length, with a 17.8 cm space between rows within the plot and 25.4 cm between plots. No plant growth hormone or foliar fungicides were applied. Preplant fertilizer of 10:10:10 was applied at 224 kg/ha (22.4 kg ha^{-1} N) and followed by a top dress in the spring of 67 kg ha^{-1} N via liquid UAN 30. The spring applied herbicide regime in 2022 consisted of Harmony (35 g ha^{-1}), bromoxynil (BROX-2-EC at 1.5 L ha^{-1}) and Induce surfactant (0.7 L ha^{-1}). Herbicide applications in the spring of 2023 consisted of Axial XL (1.2 L ha^{-1}), Harmony Extra SG (35 g ha^{-1}) and Induce surfactant (0.7 L ha^{-1}). No foliar fungicide was applied.

2.1.3 Trait phenotyping

Scald infections relied on the natural inoculum present at each field site. The scald susceptible cultivar 'KWS Scala' was planted in each block of each experiment and acted as a susceptible check and spreader ensuring adequate conidial inoculum across the trial. Plots were scored for scald symptoms at approximately Feekes stage 11.1 to 11.3 on June 13th and 9th in 2022 at the Helfer Farm and Snyder Farm field sites, respectively, and at Feekes stage 11.1-11.3 from June 26th to the 30th, and June 15th to 19th in 2023 at the McGowan Farm and Ketola Farm field sites respectively. Plots were scored on a 0-9 scale in all four environments. Severity was also scored as a percentage diseased leaf area (DLA) for the upper canopy in 2023. 2022 trial scores were converted to a % DLA. Additional agronomic traits were scored in the trials including winter survival (WS), measured as percentage of plants surviving taken in the early spring; heading date (HD), when 50% of the heads had completely emerged from the sheath (converted to Julian heading date); and plant height, measured as the height (HT) from the ground to the top of the spike excluding awns.

2.1.4 Data analysis

The scald DLA, WS, HD and HT were analyzed separately in 2024 JMP® 17.1 (JMP Statistical Discovery LLC, Cary NC) using a mixed model (restricted maximum likelihood; Reml) with genotype as fixed effects, and environment, row within environment, and column within environment as random model effects. Least squared means were used to determine frequency distributions and parental phenotypic value in comparison to the population. Spearman's correlations between DLA, WS, HD, and HT were determined using JMP. Heritability was determined on an entry-means basis where $h^2 = \sigma^2_g/(\sigma^2_e/t + \sigma^2_g)$, with σ^2_g, and σ^2_e representing genetic variance, and experimental error, respectively, and t representing number of test environments (Fehr, 1987).

To normalize the residuals and homoscedasticity for association analysis, the DLA, WS, HD, HT measurements were analyzed in a simple linear model in R to estimate the residual parameters for the population of 377 without controls, with model effects of genotype, environment, row within environment and column within environment as fixed effects. A constant of 1 was added to each DLA measurement to avoid nulls for transformation. The best lambda for transformation of the data was determined using the Box-Cox function (Box & Cox, 1964) in the MASS package in R v3.2.3 (R Core Team, 2015), that was used to transform for normal residuals and homoscedasticity. The DLA (with added constant of 1), WS, HD and HT were transformed using respective lambda values of -0.1818, 2.9494, -7.0303 and 0.0606 for DLA, WS, HD and HT, respectively. The HD transformed data was multiplied by 1×10^{16} for further analysis.

The best linear unbiased predictors (BLUPs) transformed DLA scores were estimated using Reml in JMP with WS, HD and HT as fixed covariate effects and genotype, environment, row within environment, and column within environment as random effects. The BLUPs for the transformed values for DLA, WS, HD, and HT were also calculated using Reml in JMP with genotype, environment, row within environment and column within environment as random effects.

2.2 Genotypic Analysis

2.2.1 SNP Genotypic Data

Plant tissue was harvested from the multiparent population at the two-leaf stage. Tissue was lyophilized and a modified Cetyltrimethylammonium bromide (CTAB) extraction was used for DNA extraction (Doyle & Doyle,1987). DNA was genotyped with the 50K Illumina iSelect SNP array (Bayer et al., 2017; Mascher et al., 2017, 2021) at the USDA-ARS North Central Small Grains Genotyping Lab in Fargo, ND and resulted in high quality SNP data for 374 lines. The SNP data was trimmed from the original 43078 SNPs to exclude homozygous SNPs across the population using Tassel5.0 (Bradbury et al., 2007). The 15,463 SNPs were used to estimate population structure.

2.2.2 Marker Genotypic Data

Leaf tissue was collected for specific marker traits associations (MTA) within known resistance and/or height genes. For the MTA analysis, three kernels per line included in the multiparent population were planted in a 96 cell tray and grown under a light bench. Tissue was harvested at the seedling stage and lyophilized. The modified CTAB extraction was used to extract DNA (Doyle & Doyle, 1987).

248 The multi-parent population was genotyped for the plant height gene, *HvGA20ox2*, also known as *semi-*
249 *dwarf1* (*sdw1*), to test for the presence of the *sdw1.d (Diamant)* or *sdw1.c* (denso) alleles (Xu et al.,
250 2017). The *sdw1.d* and *sdw1.c* alleles were amplified via polymerase chain reaction using mutant
251 specific primers based on Xu et al. (2017), with the adaptation of a fluorescent M13-tail in the forward
252 primers for both the sdw1.d allele (5401F_M13F; 5'- TGTAAAACGACGGCCAGTGGTGCTCCAGACCGCTCAG-
253 3') and sdw1.c (MC40861P3F_M13F; 5'- TGTAAAACGACGGCCAGTTATGGCGTGACCAAAGGTTC-3') that
254 correspond to the reverse primers for *sdw1.d* (5549R; 5'-CGGCGGAGGGGTCAATG-3'), and *sdw1.c*
255 (MC40861P4R; 5'- CACCAATCCACCACGAAGA-3'). The PCR reaction consisted of ~30 ng genomic DNA,
256 12.5 µl of GoTaq polymerase, 0.8 µM M13F primer, 6 µM R primer, 6 µM M13-FAM primer (*sdw1.d*) or
257 M13-VIC primer (*sdw1.c*) and 8.22 µl of H_20 in a 25 µl reaction. The PCR amplification protocol for the
258 *sdw1.d* primer pair included an initial denaturation step of 94°C for 3 m, 30 cycles (94°C for 1 m, 55°C for
259 30 s, 72°C for 30 s), 10 cycles (94°C for 1 m, 50°C for 30 s, and 72°C for 30 s), and a final extension cycle
260 of 72°C for 20 m. The PCR amplification cycle for the sdw1.c was similar to above, however the
261 annealing temperatures in the two cycles were 54°C and 53°C. Fragment analysis was performed on
262 pooled samples by the Biotechnology Resource Center (BRC) Genomics Facility (RRID:SCR_021727) at
263 the Cornell Institute of Biotechnology *(http://www.biotech.cornell.edu/brc/genomics-facility*) on an
264 Applied BioSystems 3730xl (Thermo Fisher Scientific, Waltham, MA), with the ABI 500LIZ size
265 standard. Results were analyzed in Genemarker (SoftGenetics, LLC, State College, Pennsylvania).

266 In addition, the HVS3 SCAR marker (Genger et al., 2003) was screened in the parental lines and
267 multiparent population using ~20ng genomic DNA, 1X GoTaq ® Green Master Mix (Promega Cooperation,
268 Madison, WI), 5µM Forward primer (5'-AAT CCT ACC TAT CCC ACC TT-3'*)*, 5 µM Reverse primer (5'-TAT
269 TTT CAG CCT TGT TCG GC-3') in a final reaction volume of 25 µl. The DNA was amplified via PCR using an
270 initial step of 94°C for 3 m, 35 amplification and extension cycles (94°C for 30 s, 50°C for 30 s, 72°C for 1
271 m), followed by a final extension cycle of 72°C for 20 m. The PCR products were amplified on a 2%
272 agarose gel using GelRed ® Nucleic Acid Stain (Biotium, Inc, Freemont, CA) for verification of PCR on a UV
273 lightbox.

274 ## 2.3 Genome-wide association analysis

275 ### **2.3.1 Genome-wide association mapping for resistance to scald with multiple models**

276 Association analysis was used to identify regions of the genome that conferred resistance to the scald
277 pathogen in our adapted germplasm. Phenotypic data included the transformed DLA, WS, HD and HT
278 BLUPs. Of the diallel population, 374 lines were used that included both genotypic and phenotypic data.
279 The 43,078 SNPs (Morex version 3) derived from the 50K Illumina iSelect SNP array (Bayer et al., 2017;
280 Mascher et al., 2017, 2021) were filtered to exclude homozygous SNPs across the population in TASSEL
281 5.0 (Bradbury et al., 2007).

282 Genome-wide association for Box-Cox transformed DLA BLUPs for scald that included WS, HD and HT as
283 covariates as previously described was ascertained using GAPIT version 3 (Wang & Zhang, 2021) in R
284 Studio (RStudio 2025.09.1+401, Posit Software, PBC). The Mixed Linear Model (MLM), Multiple Locus
285 Mixed Linear Model (MLMM), Fixed and random model Circulating Probability Unification (Farm CPU)
286 and (Bayesian-information and Linkage-disequilibrium Iteratively Nested Keyway (BLINK) models (Yu et
287 al., 2006; Zhang et al., 2010; Segura et al., 2012; Liu et al., 2016; Huang et al., 2019), using the 15,463
288 SNPs, were used to estimate marker trait association parameters for resistance to scald. Kinship and

principal component analysis (PCA) were determined within GAPIT version 3 to be used in the appropriate models. The Bonferroni threshold (Bonferroni, 1936) was used as an initial default significance threshold for R^2 (MLM) and Percent Variation Explained (PVE; MLM, MLMM, FarmCPU, and BLINK). The resulting Quantile-Quantile (QQ) plots and contributing PVE were examined to determine the appropriate GWAS model for this structured population. To reduce type 2 false negative errors due to the conservative nature of the Bonferroni threshold, the QQ plots were examined to determine the best GWAS fit that combined the reduction of spurious associations and putative significant or strong associations. The MLMM, FarmCPU and BLINK GWAS model QQ plots showed a *p*-value differentiation at the $-\log_{10}(p) = 4.2$. To determine the appropriate R^2 (MLM only) and PVE (MLM, MLMM, FarmCPU and BLINK models) the 'N.sig = n' prompt was used in GAPIT version 3 for the significance threshold where 'n' equals the number of markers for each model equal or above the $-\log_{10}(p) = 4.2$ threshold. An additional association analysis using FarmCPU with PCA = 2 as a covariate was used to validate model selection with or without PCA.

2.3.2 The *Rrs1* gene complex

Linkage disequilibrium (LD) surrounding the two strongest SNP associations identified on chromosome 3H at 172 Mbp and 442 Mbp were analyzed to determine if they were the same peak or independent associations. The LD was first assessed in TASSEL 5.0 (Bradbury et al., 2007) between the SNP at 172 Mbp and all the other SNPs on chromosome 3H (Figure 3A), and between the SNP at 442 Mbp and all the other SNPs on chromosome 3H. The Manhattan plots for the GWAS MLM model (Figure 2) were overlaid with LD estimates and used to confirm the presence of a large linkage block across the centromeric region of chromosome 3H, as visualized in the 'ggplot2' package of R v3.2.3 (R Core Team, 2015). The GWAS MLM model was used to assess associations using GAPIT version 3, using the same methodology as above, except for only using the 354 lines in the GWAS model and using the HVS3 marker data as a covariate (Figure 3C).

2.3.3 GWAS for resistance to scald, winter survival, heading date and plant height

The Box-Cox transformed DLA BLUPS (without WS, HD, and HT as covariates), as well as Box-Cox transformed WS, HD, and HT BLUPs were used as independent trait variables in both MLM and FarmCPU analysis using GAPIT version 3 in RStudio, with the 15,463 SNPs. The significant thresholds were based on visual inspection of the QQ plots of FarmCPU and set to $-\log_{10}(p) = 4.0$. As in the first GWAS analysis listed above, the models were run again using the 'N.sig = n' prompt to determine the correct PVE in GAPIT version 3. The resulting Manhattan plots were created in ggplot2 in RStudio.

The LD along chromosome 2H was compared to the significant SNP in the marker-trait association for resistance to scald, to determine if there was co-localization and/or LD between WS, HD, and HT to resistance to scald. The Manhattan plot was created in ggplot2 to map the LD and SNP marker trait associations from the MLM GWAS model, and included the clustered SNP regions of the WS, HD and HT marker trait associations on the short end of chromosome 2H. Regions around the DLA, WS, HD and HT SNP associations were based on the SNP associations in the MLM model that were above $-\log_{10}(p) = 4.0$, as an indicator of the confidence interval for the trait.

3 RESULTS

3.1. The multi-parent population pedigree

The genetic population used in this dataset is structured as an unbalanced diallel design derived from 377 biparental crosses between four winter malting barley cultivars ('Flavia', 'KWS Scala', 'SY Tepee', and 'WintMalt') and one facultative malting barley cultivar ('Lightning'; Figure 1). The largest number of lines was derived from 'Lightning' x 'SY Tepee' crosses, with 93 lines. 'Lightning' was the parent with the most lines represented, with 272 (72%) of the 277 lines. 'WintMalt' was the parent with fewest lines represented with only 95 of the 377 lines (25%). The fewest number of lines were from the cross between 'WintMalt' x 'SY Tepee', with four lines. Additional parents were present in the population with 43.8% (165 lines), 35% (132 lines), 26% (100 lines) for 'SY Tepee', 'Flavia', and 'KWS Scala' respectively.

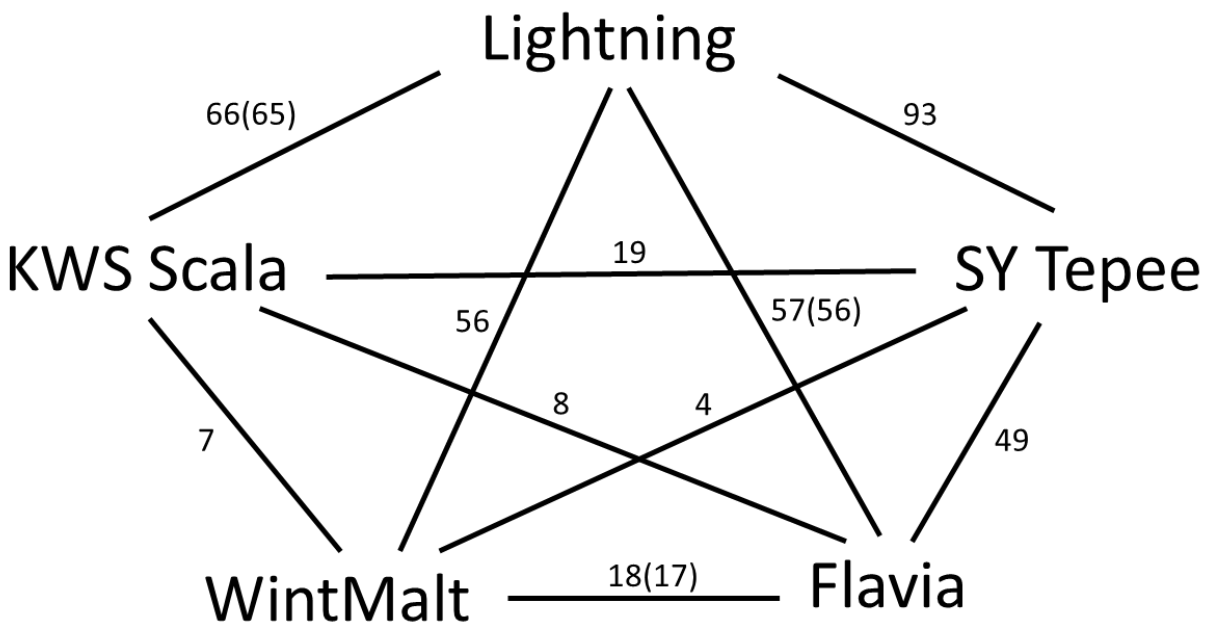

Figure 1. Structure of the unbalanced diallel multiparent population derived from five adapted cultivars. The 377 lines consisted of recombinant inbred lines and doubled haploids. The number of lines between each biparental cross is indicated along the line between the two parents, which were used for statistical analysis (377 lines) and for GWAS analysis (374 lines) with three lines less as indicated by the numbers in parenthesis.

3.2 Segregation for disease and agronomic traits in the multiparent population

The multi-parent population along with the corresponding parental cultivars, additional breeding lines and several check cultivars were grown in four environments at the Cornell University Campus Area Farms near Ithaca, NY, including two field sites (Helfer Farm and Snyder Farm) in 2022, and two field sites (McGowan Farm and Ketola Farm) in 2023 (Supplemental Table S1). *A priori* knowledge of these field sites indicated a historical presence of the scald pathogen in each environment. To ensure adequate disease development in the field as well as monitor disease, the scald susceptible variety 'KWS Scala'

(Blachez et al., 2018) was grown in each experimental block, ranging from 13 entries in the Helfer Farm, 2022 field site to 17 entries in the McGowan Farm 2023 field site.

Distributions of disease and agronomic traits showed transgressive segregation for most traits from the parental lines. The distribution of scald DLA was skewed towards the y-axis, with Lighting as resistant, 'SY Tepee' as moderately resistant, and 'WintMalt', 'KWS Scala' and 'Flavia' as susceptible to scald (Supplemental Fig1). An analysis of variance indicated significant variation for DLA for genotypes, environment and rows within environment. The means and ranges of disease severity within the 377 lines grown across the locations varied with 50.8% (0-99%) in Helfer Farm, 2022, 19.9% (0-99%) in Snyder Farm, 2022, 6.0% (0-90%) in Ketola Farm, 2023, and 19.7% (0-95%) in McGowan Farm, 2023.

Across all three agronomic traits, significant variation was identified for genotype, rows within environment, and columns within environment, but not between environments. Across the four environments, WS was skewed towards 100% survival, with 'SY Tepee', 'WintMalt' and 'KWS Scala' showing good winter survival (>85%). 'Lightning' and 'Flavia' showed moderate winter survival (~75-80%), while a check cultivar, 'Endeavor', showed poor winter survival. The average winter survival within the population ranged from 75% (Helfer Farm, 2022) to 87% (Ketola Farm, 2023) with an average across the four environments of 79.9%. Differences in heading date between the parents ranged from ~143 days (Flavia) to ~151 days ('WintMalt'), with 'Lightning', 'SY Tepee' and 'KWS Scala' showing mid-range heading dates between 145 days to 147 days. The heading date (Julian) ranged from an average of 142 days in McGowan Farm, 2023 to 150 days to heading in Helfer Farm, 2022. Plant height ranged from an average of 52 cm to 67 cm in Ketola Farm, 2023 (Supplemental Table S1 & S2). Heritability based on an entry-means basis for DLA, WS, HD and HT were 0.76, 0.69, 0.83 and 0.57 respectively.

3.3 Scald is correlated with agronomic traits

Correlations between scald DLA and agronomic traits were ascertained to determine the effect of winter survival, heading date and plant height on scald using the 377 lines within the multiparent population (Supplemental Table S2). A highly significant negative correlation was identified between DLA and plant height ($P < 0.0001$; $R^2 = -0.29$), indicating that taller plants had less disease in the upper canopy. A significant correlation was also identified between heading date and scald DLA ($P < 0.0107$; $R^2 = 0.13$), indicating that a later heading date had more DLA. The correlation between winter survival and DLA was not significant across environments ($P = 0.1065$). Notably, there was a significant interaction between

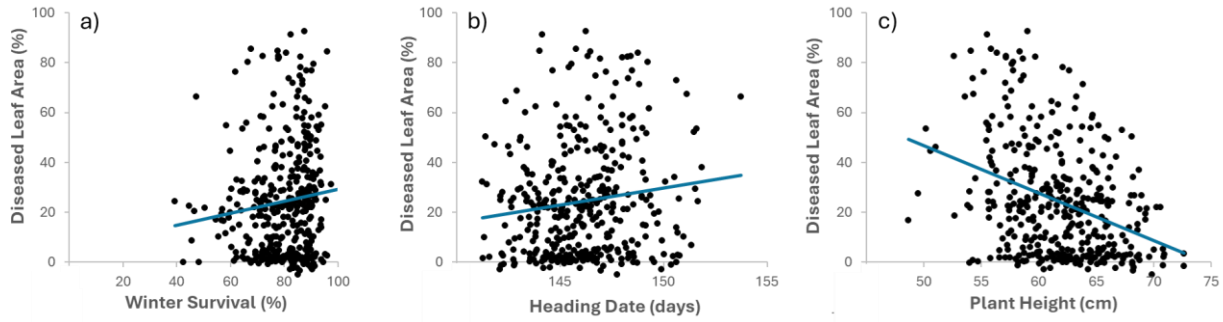

Figure 2. Spearman's correlation between resistance to scald (diseased leaf area), and a) winter survival, b) heading date and c) plant height, in the 377 line multiparent population across four environments in 2022 and 2023.

winter survival and heading date (P=0.0229; R^2 = -0.1171), and a highly significant interaction between WS and plant height (P<0.0001; R^2 = 0.38), and no significant correlation between heading date and plant height.

3.4 Genome wide association mapping for resistance to scald

3.4.1 GWAS for resistance to scald using multiple GWAS models

Population structure determined via principal component analysis in GAPIT version 3 (Wang & Zhang, 2021; Supplemental Figure S2) indicated that the multiparent population consisted of four groupings with the use of only the first and second PCAs, indicative of the relatedness between RILs and DHs. The QQ plot of the MLM GWAS model showed marked deviation of the observed from expected *p*-values for the MLM model that accounts for both population structure and kinship (Figure 3). The MLMM, FarmCPU and Blink models had QQ plots that were largely in line with the observed and expected *p*-values. The FarmCPU model with PCA = 2 as a covariate resulted in a QQ plot with the observed $-\log_{10}(p)$ values skewing towards the x-axis in comparison to the FarmCPU model with no PCA covariate and was not further pursued (Supplemental Figure S3). The Bonferroni threshold of $-\log_{10}(p) = 5.5$ was initially used in GAPIT version 3 as the default to determine significance. Analysis of the QQ plots, and particularly the QQ plots from the FarmCPU analysis, showed that a threshold of $-\log_{10}(p) = 4.2$ was more appropriate and reduced type II errors, where the observed veered from the expected regression line. Re-analysis of the GWAS models for MLM, MLMM, FarmCPU and Blink threshold set to $-\log_{10}(p)$ of -4.2 was used to estimate the appropriate phenotypic variation explained (Table 1) and showed distinct differences between models (Supplemental Table S3 & S4).

MLM: The mixed linear model, with population structure and kinship included, resulted in 77 SNPs associated with resistance to scald (Figure 3). Seventy-seven SNPs were localized in two SNP clusters on chromosome 3H and spanned a region from 88 Mb to 448 Mb. Two peaks across this region were identified as the significant associations, with the most significant SNP association located at 174,868,558 bp, with a $-\log_{10}(p) = 7.3$ (MAF = 0.46; PVE = 0.6%. The second SNP peak was located at 442,185,927 bp, with a $-\log_{10}(p) = 7.0$ (MAF = 0.47; PVE = 3.8%). An additional SNP association was identified on chromosome 6H (MAF = 0.004; PVE = 50.9%). Despite the large phenotypic variation attributed to the SNP association on chromosome 6H, it appears to be an anomaly (false positive) and will be treated as such in the further interpretation of results.

MLMM: Using MLMM, two SNPs were found to be associated with resistance to scald (Figure 3). The single peak identified was located on chromosome 3H, at 174,868,558 bp, with a-$\log_{10}(p) = 11.1$ (MAF = 0.46; PVE = 19.4%). The second association was identified as a false positive at the previously described SNP on chromosome 6H: 65,563,245 bp (MAF = 0.004; PVE = 51.6%).

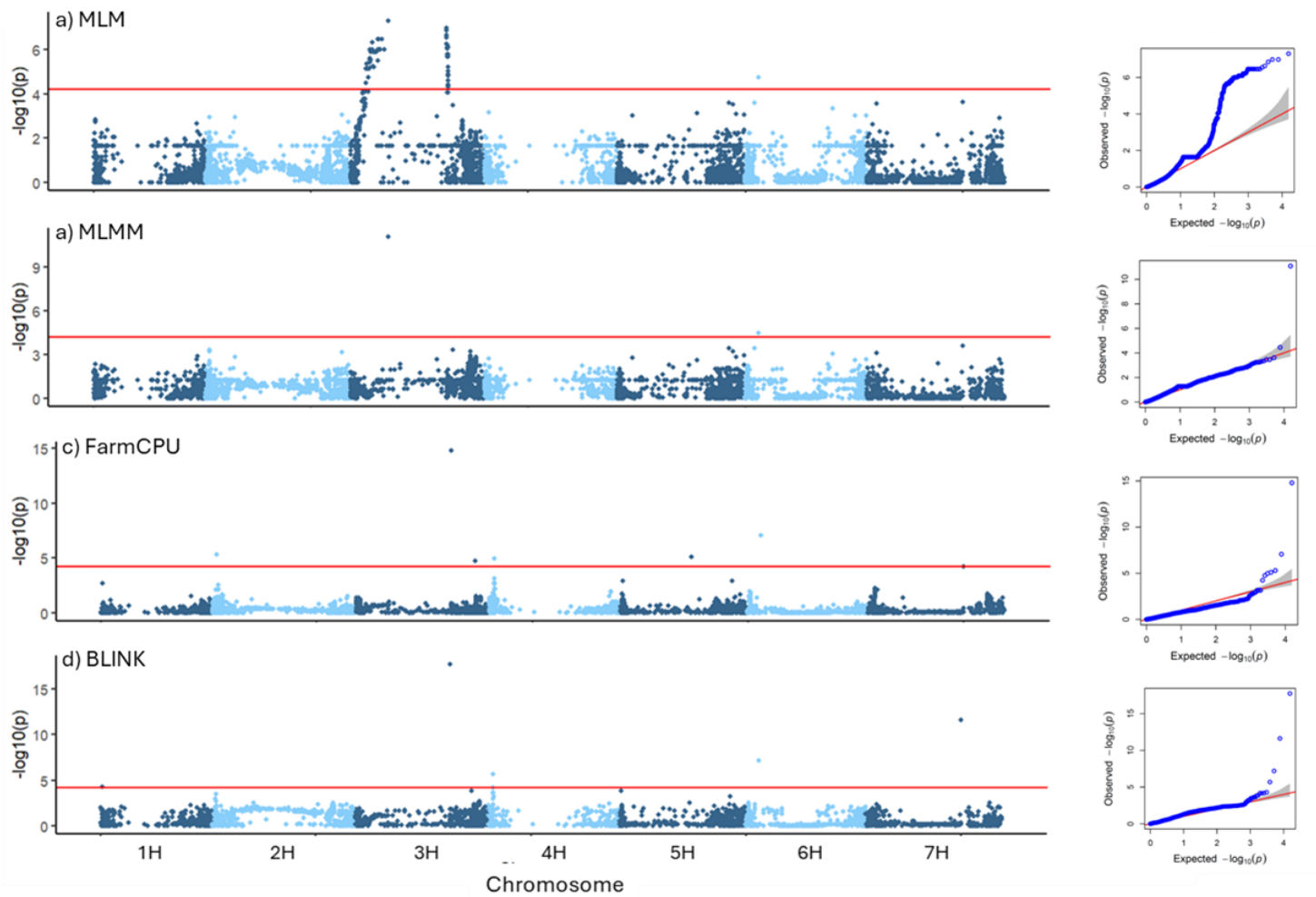

Figure 3. Manhattan plots of the GWAS models including a) MLM, b) MLMM, c) FarmCPU, and d) BLINK, with corresponding QQ plots (right) in GAPIT version 3 for resistance to scald in the multiparent population with using DLA BLUPs for resistance to scald. DLA BLUPs for resistance to scald were calculated using winter survival, heading date and plant height as covariates in the BLUP model in four environments across 2022 and 2023. The red horizontal line in the Manhattan plots indicate the QQ plot - determined threshold of $-\log_{10}(p)$ of 4.2.

425 *FarmCPU:* The FarmCPU model identified four SNPs associated with resistance to scald (Table 1). The
426 most significant SNP was located on chromosome 3H at 442,185,927 bp with a $-\log_{10}(p) = 14.8$ (MAF =
427 0.47; PVE = 27.1%). The SNP association on chromosome 2H was at 18,144,981 bp (MAF = 0.426; PVE =
428 8.1%) Additional SNP associations were identified on chromosomes 3H (553,288,836 Mbp; MAF = 0.303;
429 PVE = 5.2%), 4H (MAF = 0.240; PVE = 0.8%). Two additional SNP marker trait associations were identified
430 however both had low MAF and are considered aberrations, including the association on chromosome
431 6H at 65,635,245 bp (MAF = 0.004; PVE = 6.3%) and on chromosome 5H at 329,813,939 bp (MAF =
432 0.021; PVE = 2.8%). FarmCPU with PCA=2 resulted in a QQ plot with the observed $-\log_{10}(p)$ values below
433 the expected $-\log_{10}(p)$ values and skewed towards the x-axis and was not considered further
434 (Supplemental Figure S3).

435 *BLINK:* BLINK identified three SNPs associated with resistance to scald. The most significant SNP was
436 located on chromosome 3H: 442,185,927 bp, with a $-\log_{10}(p) = 17.7$ (MAF = 0.47; PVE = 7.6%). The next
437 most significant SNP was located on chromosome 7H: 443,811,200 bp with a $-\log_{10}(p) = 11.6$ (MAF =
438 0.327; PVE = 9.0%). The third SNP marker trait association was found on chromosome 4H at 22,416,684
439 bp with a $-\log_{10}(p) = 5.7$ (MAF = 0.24; PVE = 4.3%). As with the other models, a SNP association was
440 identified on chromosome 6H: 65,635,245 bp with a $-\log_{10}(p)$ of 7.2 (MAF = 0.004; PAV = 62.6%) and is
441 considered an aberration.

442 A discrepancy between the GWAS models was identified, that was important in interpreting how to
443 proceed with the analysis. The difference in SNP marker trait associations between the MLM, MLMM,
444 FarmCPU and BLINK spans both SNP location and effect size. Notably, there appeared to be two large
445 peaks on chromosome 3H (MLM) that were either an association on the first peak (MLMM) or on the
446 second peak (FarmCPU; BLINK). In addition, PVE for the large peaks on chromosome 3H (442 Mbp)
447 varied , with FarmCPU providing a PVE = 27%, indicative of a major gene such as the *Rrs1*, which co-
448 localizes to that region.

449 Using Tassel 5.0 (Bradbury et al., 2007), the LD along chromosome 3H was compared to both peaks
450 separately (Figure 4). Using the SNP at 174,868,558 bp, the LD analysis showed that SNPs across both
451 peaks were in LD with the peak at 174 Mb, indicating a large linkage block that spanned the centromere.
452 The LD analysis comparing the SNPs at the second peak at 442,185,927 bp also indicated that SNPs
453 across both peaks were in LD with the second peak. In both scenarios of GWAS using MLM, where both
454 peaks presented as being associated with resistance, the LD patterns were tightly linked and in
455 coordination with the *p*-values of the surrounding SNP association landscape. As this population is
456 derived from recombinant inbred lines and/or doubled haploids, it appears that the two large peaks on
457 chromosome 3H comprise one large linkage block that spans the centromere. The SNP at 442 Mb is also
458 the most significant SNP identified via GWAS MLM, and in FarmCPU and BLINK, with FarmCPU indicating
459 the most variation explained by this SNP.

460 **3.4.2 *Rrs1* is segregating in a large linkage block on chromosome 3H**

461 The cluster of SNPs with high marker-trait associations on chromosome 3H co-localized near the *Rrs1*
462 locus. To determine if the resistance in this region is due to the major resistance gene complex, *Rrs1*, the
463 population was scored for the HVS3 SCAR marker, located downstream of the *Rrs1* gene (Genger et al.,
464 2003). 'Lightning' harbored the resistance allele at 250 bp, while 'Flavia', 'KWS Scala', 'SY Tepee' and
465 'WintMalt' carried the susceptible allele at ~500 bp. (Supplemental Table S5). The HVS3 marker was

466 used as a covariate in both the MLM and FarmCPU GWAS analysis in GAPIT version 3. The resulting
467 Manhattan plot along chromosome 3H (Figure 4c) indicates the collapse of the entire region of SNP
468 associations to well below the threshold level, indicating the resistance identified via GWAS model is
469 conferred via *Rrs1*. Using the HVS3 marker as a covariate in the GWAS model implies *Rrs1* as the
470 resistance mechanism across this large region.

471 Based on the Morex version 3 genome, the SNP at 442,185,927 bp was located within a receptor-like
472 kinase (HORVU.MOREX.r3.HG0281210.1), that is one of several kinase and receptor-like kinase genes
473 clustered in the region. The SNP located on chromosome 3H at 553,288,836 bp co-localized with the
474 *Rrs4* gene (Patil et al., 2003), located at 576.6 Mbp. The SNP resides in a Protein 1Q-Domain 1 gene
475 (HORVU.MOREX.r3.3HG0303590.1). The *Rrs17* resistance gene is located at 10.4 Mbp (Wagner et al.,
476 2008), upstream of the SNP identified on chromosome 2H located at 18.1 Mbp, that is located within a
477 leucine-rich repeat receptor-like protein kinase (HORVU.MOREX.r3.2HG0104570). The identified SNP on
478 chromosome 4H at 22,416,684 bp is located within HORVU.MOREX.r3.4HG0338290, a glucan endo-1 3-
479 beta glucosidase gene.

480 Table 1. SNP-trait associations for resistance to scald using DLA BLUPs (using winter survival, heading date and plant height as covariates in the
481 BLUPs), 374 lines and 15,463 SNPs in the MLM, MLMM, FarmCPU and BLINK GWAS models using a threshold of $-\log_{10}(p) > 4.2$.

SNP Marker Name	Chromosome	Position (bp)[a]	*p-value*	MAF[b]	Allele	Effect[c]	Phenotype Variance Explained (%)
MLM							
JHI-Hv50k-2016-168548	3	174,868,558	5.00E-08	0.462	c/t	-0.0398	0.6
JHI-Hv50k-2016-183351	3	442,550,473	2.35E-07	0.473	c/t	-0.0380	3.8
JHI-Hv50k-2016-183207	3	442,203,921	1.05E-07	0.471	t/a	-0.0380	0.7
SCRI_RS_221644	3	442,185,927	1.05E-07	0.471	a/g	-0.0380	0.1
JHI-Hv50k-2016-166941	3	127,232,535	3.47E-07	0.460	t/c	0.0005	0.0
MLMM							
JHI-Hv50k-2016-168548	3	174,868,558	8.22E-12	0.462	**c**/t	-0.0412	19.4
FarmCPU							
SCRI_RS_221644	3	442,185,927	1.58E-15	0.471	a/g	-0.0319	27.1
JHI-Hv50k-2016-70026	2	18,144,891	5.03E-06	0.426	g/a	-0.0121	8.1
JHI-Hv50k-2016-232214	4	22,416,684	1.04E-05	0.240	a/t	0.0130	0.8
JHI-Hv50k-2016-202358	3	553,288,836	1.76E-05	0.303	t/c	0.0130	5.2
BLINK							
SCRI_RS_221644	3	442,185,927	1.81E-18	0.471	a/g	-0.0335	7.6
JHI-Hv50k-2016-514374	7	443,811,200	2.39E-12	0.327	g/n	-0.0551	9.0
JHI-Hv50k-2016-232214	4	22,416,684	2.05E-06	0.240	a/t	0.0113	4.3

482 [a] SNP position based on Morex version 3 (Mascher et al., 2021)
483 [b] MAF, minor allele frequency
484 [c] Effect is based on Box Cox transformed data and as a result is a) not directly transferrable to unit measurements of DLA and b) the negative Box
485 Cox transformation of DLA results in the reverse effect direction of the DLA effect.

486

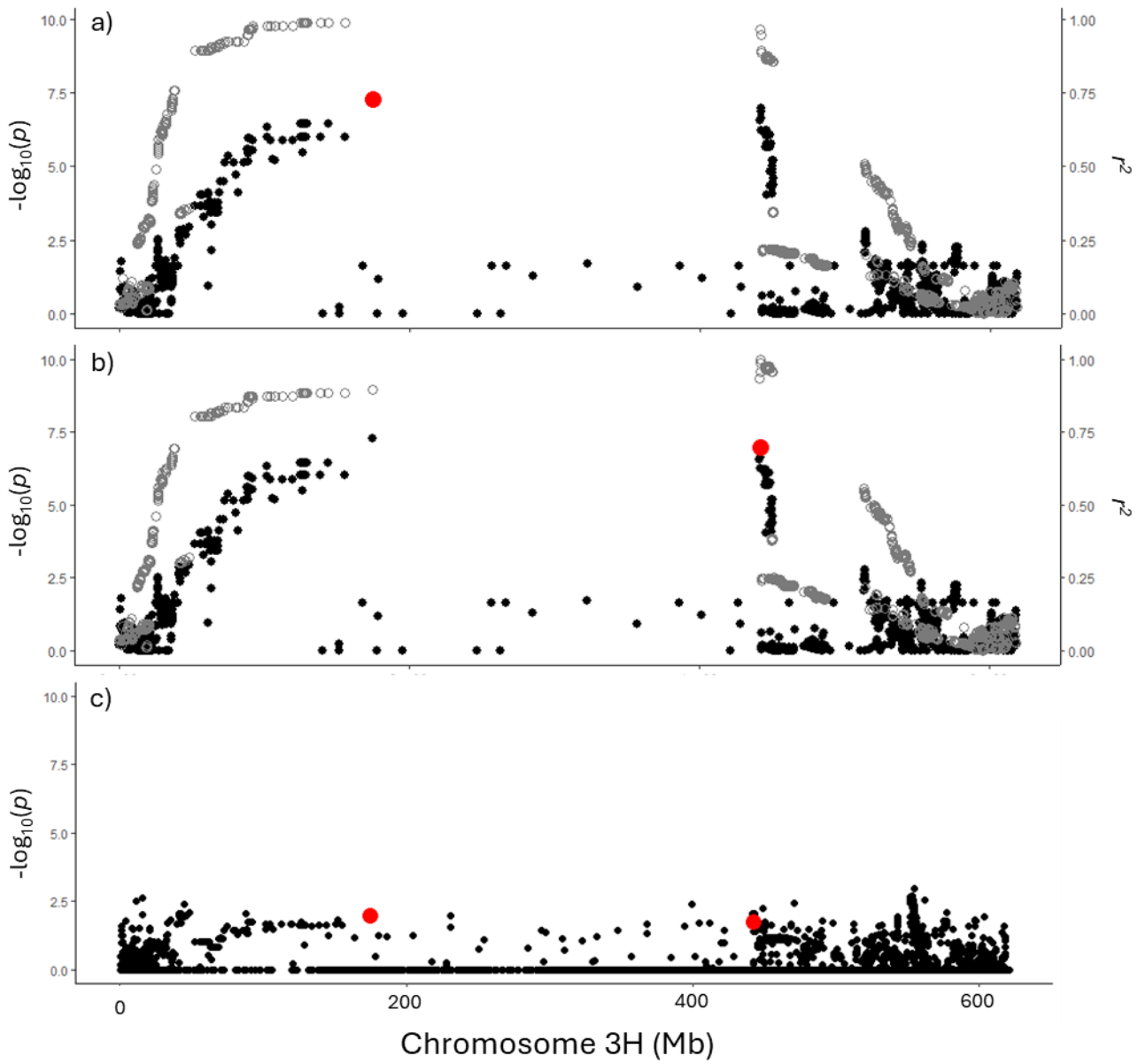

Figure 4. Dissection of the SNP-trait association (MLM) cluster on chromosome 3H for resistance to scald DLA, where a) characterizes linkage disequilibrium (LD) in relation to the first SNP trait association at 174 Mbp, b) characterizes LD in relation to the second SNP-trait association at 442 Mbp, and c) the Manhattan plot shows SNP-trait associations across chromosome 3H using the MLM GWAS model in GAPIT version 3 using the HVS3 (*Rrs1*) scar marker as a covariate). SNP associations are labeled as black dots. Linkage disequilibrium indicated as R^2 is shown in grey dots in a) and b). The most significant SNP-trait association at 174 Mbp and 442 Mbp chromosome 3H are indicated as red dots in all three panels.

Four GWAS models were used to validate SNP associations across the genome for resistance to scald. All four models have different approaches for estimating associations and are available to avoid overfitting analysis. The most significant SNP association(s) in this study resided on chromosome 3H at either 174.8 Mbp or 422.1 Mbp. FarmCPU and Blink associations at these peaks had the lowest *p*-values (i.e., the

499 most significant) across the models. Importantly, the PVE greatly differed between the models for these
500 two SNPs. The PVE at 174.8 Mbp ranged from 0.6% to 19.4% for MLM and MLMM, respectively. The
501 PVE at 442.1 Mbp was 0.1%, 27.1% and 7.6% for the MLM, FarmCPU and Blink models, respectively. The
502 FarmCPU model PVE of 27.1% is indicative of major gene resistance such as *Rrs1*. The SNP association
503 on chromosome 6H, explained ~50% of the phenotypic variation in MLM, MLMM, and BLINK despite the
504 very low MAF (0.004) and given the variation in the few SNPs at this locus, appears to be a type I error.
505 The FarmCPU model constrains the PVE of this SNP at 6%. Due to the PVE allocated for the *Rrs1* region,
506 as well as for the aberrant SNP on chromosome 6H, and for simplicity, the FarmCPU was the model that
507 was used in the further analysis, being considered the best fit for this population. The MLM model was
508 also used for reference.

509 **3.4.3 GWAS for resistance to scald compared to agronomic traits via FarmCPU**

510 Association analysis across disease and agronomic traits for the 374 lines was used to identify SNP
511 associations for resistance to scald, winter survival, heading date and plant height to determine if there
512 was any colocalization of marker associations that explained the phenotypic traits (Table 2). The BLUPs
513 were estimated as mentioned above and included the scald DLA BLUP estimate (without using the WS,
514 HD, or HT as covariates; Supplemental Table S3). The QQ plots for the FarmCPU analysis (Figure 5)
515 indicated an adherence of the observed to expected $-\log_{10}(p)$ values except for several SNPs at the tail of
516 the slope, as expected. The separation of the observed to expected levels at the thresholds for each of
517 the traits was analyzed separately, and based on the QQ plots, a $-\log_{10}(p) = 4.0$ was used as the threshold
518 for each trait (Figure 5).

519 DLA: In general, the SNP associations identified using the scald DLA BLUPs (without the agronomic traits
520 as covariates) using FarmCPU (Figure 5; Table 2) were similar to the previous identified SNPs (using the
521 agronomic traits as covariates; Table 1). The SNP associations using the correlated traits had slightly
522 lower *p*-values (i.e., more significant), except for the *Rrs1* region on chromosome 3H. The SNP
523 associations on chromosome 3H included the main association at 442,550, 473 bp (PAV=20.7%) and
524 553,388, 8365 (PAV = 6.2%). The same SNP associations were identified on Chromosome 2H and 4H,
525 with slightly adjusted PVE of 6.7% and 1.2%, respectively. Additionally, a SNP association was identified
526 on chromosome 7H (MAF = 0.326; PVE = 0.2%; g/n) and may be a presence/absence variation. This SNP
527 association was present in the previous BLINK analysis but was below the $-\log_{10}(p) = 4.0$ significance
528 threshold for FarmCPU. The SNP association aberrations identified in the previous analysis were also
529 identified in this analysis and not considered for further discussion based on low MAF and exaggerated
530 PVE for the SNP on Chromosome 6H.

531 Winter Survival: A SNP association was identified on Chromosome 2H, at 4,217,244 bp (MAF = 0.432;
532 PVE = 0.25%). Two additional SNPs were identified in FarmCPU that did not contribute to PVE (0%)
533 including SNPs on chromosome 1H at 9,315,052 bp (MAF = 0.161) and chromosome 5H at 84,325,845 bp
534 (MAF = 0.318), which are not considered further.

535 Heading date: The most significant SNP association with heading date co-localized at *Ppd-H1* (Turner et
536 al., 2005), on chromosome 2H at 26, 107,957 (MAF = 0.389; PVE = 18.4%). Two SNP associations were
537 identified on chromosome 1H at 9,315052 (MAF = 0.161; PVE = 13.1%) and 408,764,804 bp (MAF =
538 0.311; PVE = 9.8%). Two SNP associations were identified on chromosome 4H (558,482,572 bp) and
539 chromosome 5H (468,299,945 bp) however both contributed 0% to phenotypic variation.

540 Plant Height: Eight SNP associations were identified for HT (Table 1). The most significant SNP,
541 chromosome 2H: 10,011,392 contributes approximately 8.7% to the phenotypic variation and is
542 localized just upstream of *Ppd-H1* and the SNP association peak identified for heading date. The SNP
543 variant is g/r suggesting possible gene duplication in the region. The MLM GWAS model showed a
544 defined peak with multiple significant SNPs that are not segregating for heterozygousity (Supplemental
545 Table S6). Two SNP locations are located on Chromosome 7H at 510,346,749 (MAF = 0.083; PVE =
546 18.1%) and 568,195,700 (MAF = 0.2645; PVE = 7.5%), with the latter segregating for heterozygousity
547 indicating putative gene duplication. Four additional SNP associations were identified on chromosome
548 1H, 3H, 4H and 5H that accounted for PVE from 0.7 to 2.5%, with the chromosome 4H SNP association
549 identified as a heterozygote. The SNP association located on chromosome 3H with a PVE = 0.0% was
550 also driven by a heterozygous SNP variation and may be considered a false positive.

551 The *HvGA20ox2* gene, also known as *sdw1*, is located on chromosome 3H at 563.9 Mb and, in previous
552 GWAS studies, was suggested to contribute towards reaction of barley to scald (Looseley et al., 2018). In
553 our study, there were no SNP associations for plant height or resistance to scald located within this
554 region. The multiparent population and parental lines were genotyped using the *sdw1.d* and *sdw1.c*
555 markers (Xu et al., 2017), all of which carried the wild type allele at sdw1.

556 The correlation between resistance to scald and agronomic traits resulted in the co-localization of GWAS
557 SNP associations. The inclusion of agronomic traits in the DLA BLUPs as covariates in the initial analysis
558 (Table 1; Figure 3) appeared to lower the *p*-values for identified SNP associations and resulted in a higher
559 significance threshold in comparison to DLA BLUPs without covariates. While there was no overlap
560 between the identified SNP associations for resistance to scald (without using the agronomic traits in the
561 calculation of DLA). There were, however, distinct SNP associations on the short arm of chromosome 2H
562 for resistance to scald (chromosome 2H: 18.1 Mbp; Figure 6), winter survival (chromosome 2H: 4,2
563 Mbp), heading date (chromosome 2H; 26.1 Mbp) plant height (chromosome 2H: 10.1 Mbp), however
564 there appeared to be little genomic overlap between these peaks, as seen in the Manhattan plots for the
565 GWAS MLM model (Supplemental Fig S4). The linkage disequilibrium between the significant peak for
566 resistance to scald (DLA) and the remaining SNPs along chromosome 2H indicated that this region may
567 harbor LD, and that the scald DLA association should likely be considered a QTL related to architectural
568 avoidance (Figure 6). Alternatively, the SNP association is located within a gene encoding agmatine
569 coumaroyltransferase-2 (ACT-2), known to produce antifungal compounds (Burhenne et al., 2003). The
570 resistance gene, *Rrs17*, is also located at 10.4 Mbp (Wagner et al., 2008)

571

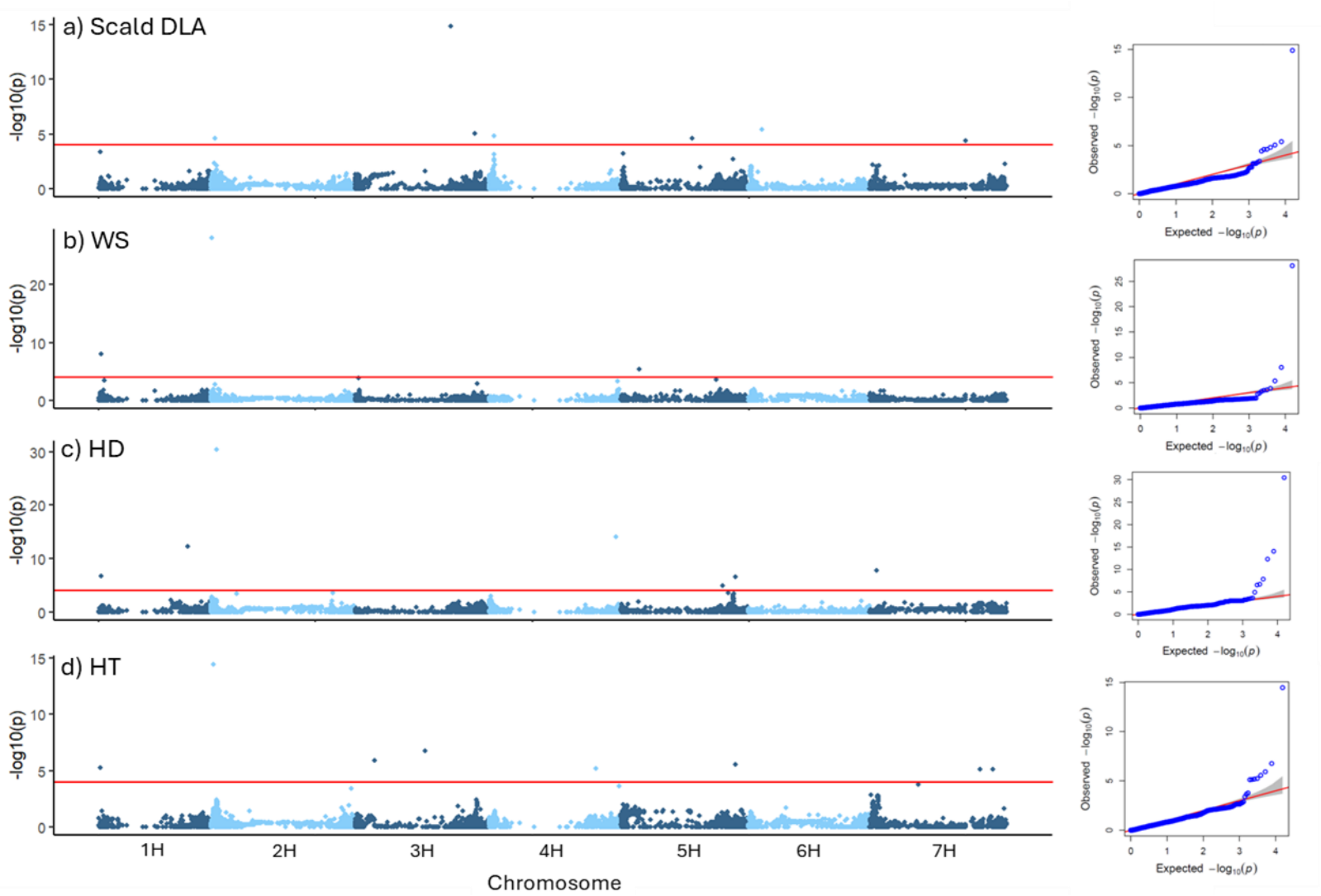

Figure 5: Manhattan plots for a) resistance to scald (DLA), b) winter survival (WS), c) heading date (HD), and d) plant height (HT) using the 374 lines and 15,463 SNPs in the FarmCPU GWAS model, and corresponding QQ plots (right). DLA BLUPs for resistance to scald were calculated without using winter survival, heading date and plant height as covariates in the BLUP model. All traits BLUPs were calculated in four environments across 2022 and 2023. The red horizontal line indicates the QQ plot – determined threshold of $-\log_{10}(p)$ of 4.0.

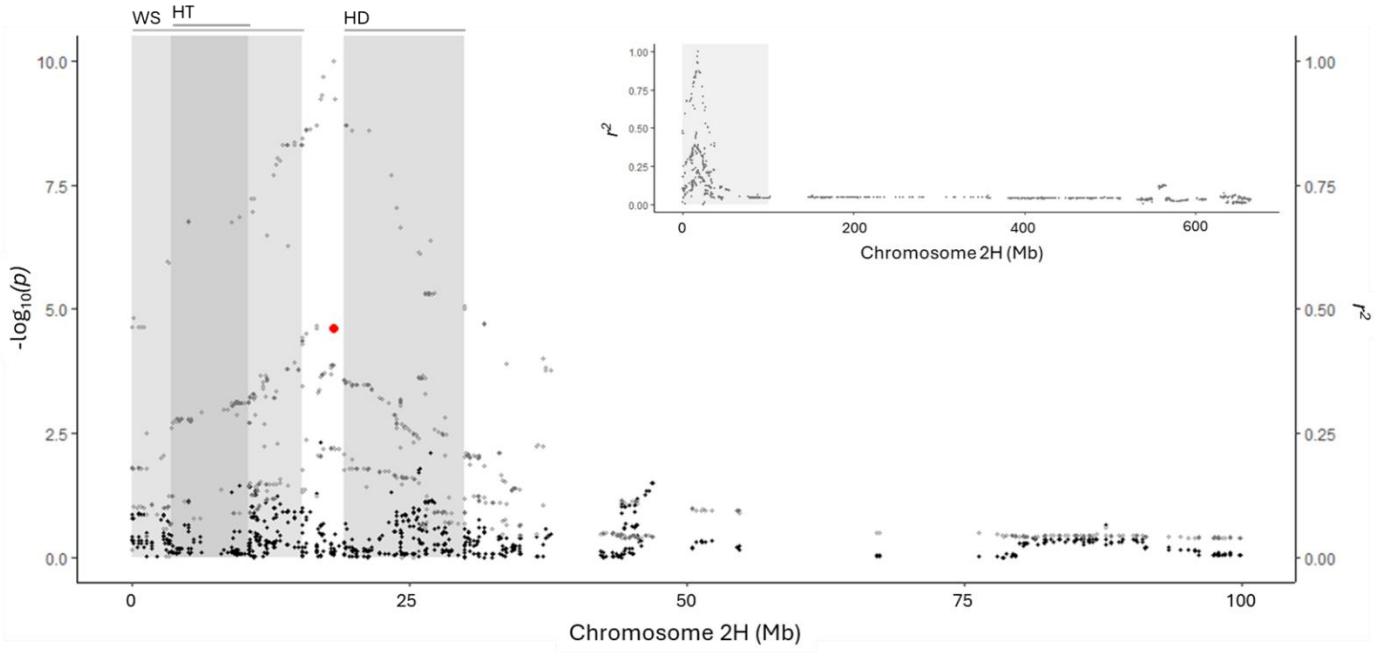

Figure 6. Association and linkage disequilibrium (LD) analysis across chromosome 2H for resistance to scald (DLA; black dots). The Manhattan plot (left y axis) with black dots depicts the SNP associations for resistance to diseased leaf area (DLA) using FarmCPU in GAPIT version 3 with the most significant SNP association identified as a red dot across the first 1 Mb of chromosome 2H. Grey vertical shaded regions in the main graph represent confidence intervals based on significant MLM associations (Supplemental Figure S) of co-localized SNP-trait association clusters for winter survival (left, grey bar), heading date (right, grey bar) and plant height (left, dark grey bar). The LD estimate scatter plot (right *y*-axis) with grey dots indicates the LD of neighboring SNPs in relation to the SNP associated with resistance to scald (in red). The top right graph insert indicates the LD across chromosome 2H with respect to the most significant associated SNP for DLA. The vertical grey shaded box indicates the 1 Mb region shown in the main graph.

591 Table 2. SNP-trait associations for diseased leaf area for scald, winter survival, heading date and plant height BLUPs, for the 374 lines and 15,463
592 SNPs in the FarmCPU GWAS model using a threshold of $-\log_{10}(p) > 4.0$. using the FarmCPU model

SNP	Chromosome	Position (bp) [a]	*p-value*	MAF[b]	Allele	Effect[c]	Phenotype Variance Explained(%)
Scald DLA							
JHI-Hv50k-2016-183351	3	442,550,473	1.28E-15	0.473	c/t	-0.0335	20.7
JHI-Hv50k-2016-202358	3	553,288,836	8.77E-06	0.300	t/c	0.0162	6.2
JHI-Hv50k-2016-232214	4	22,416,684	1.55E-05	0.240	a/t	0.0127	1.2
JHI-Hv50k-2016-70026	2	18,144,891	2.45E-05	0.425	g/a	-0.0119	6.7
JHI-Hv50k-2016-514674	7	443,811,200	3.76E-05	0.326	g/n	0.1888	0.2
Winter survival							
JHI-Hv50k-2016-61826	2	4,217,244	8.22E-29	0.432	a/g	-36892.4	0.25
Heading date							
JHI-Hv50k-2016-73663	2	26,107,957	3.59E-31	0.389	g/t	0.5854	18.4
BOPA1_4178-1592	1	408,764,804	4.96E-13	0.311	a/g	0.2405	9.8
JHI-Hv50k-2016-9518	1	931,5052	2.00E-07	0.161	a/g	-0.1999	13.1
Plant height							
JHI-Hv50k-2016-64130	2	10,119,392	3.40E-15	0.288	g/r	-0.0676	8.7
JHI-Hv50k-2016-175127	3	322,820,460	1.71E-07	0.499	c/n/y	-0.3922	2.2
JHI-Hv50k-2016-335573	5	527,330,768	2.68E-06	0.201	a/g	0.0264	2.5
JHI-Hv50k-2016-7860	1	7,633,880	5.75E-06	0.499	a/g	-0.0211	1.5
JHI-Hv50k-2016-250342	4	494,857,832	6.47E-06	0.198	g/r	0.0379	0.7
JHI-Hv50k-2016-493281	7	568,195,700	7.29E-06	0.264	a/g	-0.0261	7.5
JHI-Hv50k-2016-490693	7	510,346,749	7.53E-06	0.083	t/w	0.0507	18.1

593 [a] SNP position based on Morex version 3 (Mascher et al., 2021)
594 [b] MAF, minor allele frequency
595 [c] Effect is based on Box Cox transformed data and as a result is a) not directly transferrable to unit measurements of traits and b) the negative Box
596 Cox transformation of DLA and HD results in the reverse effect direction of effects.

4 DISCUSSION

4.1. Breeding for resistance to scald in winter malting barley is important.

Malting barley is a commercially important crop due to its value in the brewing and distilling industries. The malting process demands uniformly high quality grain. Winter malting barley, grown in New York for the craft brewing industry, faces unique challenges due to the wet humid weather in this region. Foliar fungal diseases affect both spring and winter malting barley, resulting in yield loss and kernel quality issues. The environmental conditions encountered by winter malting barley grown in New York are more conducive to scald infections than spring barley, even when grown in similar regions (Kolkman et al., 2025a, b).

In this study, ambient inoculum of *R. graminicola* was relied upon for field infections. Winter malting barley is planted in the fall and develops in the early spring season in New York when weather is favorable for development, reaching levels of up to 77% severity in susceptible germplasm (Kolkman et al., 2025a). The distribution of the susceptible parent check, 'KWS Scala', across each of the environments in this study validated the consistent natural infection across the experiment, while early season infections in 'KWS Scala' provided spore production across the experiment that resulted in consistent disease severity in highly susceptible genotypes.

4.2 Resistance in the multiparent population is comprised of both major resistance genes and quantitative disease resistance.

The *Rrs1* gene complex is an important source of resistance to scald. We identified a large linkage block on chromosome 3H that spanned the centromere and initially appeared as two separate peaks in the MLM GWAS model. Linkage disequilibrium analysis validated that the large region was in LD with the most significant peak that co-localized near the *Rrs1* gene complex. Additional evidence of the large linkage blocks was seen in the deviation of the observed: expected *p*-values as seen by the heavily skewed slope in the QQ plots for the GLM and MLM models. The evidence of a large linkage block at *Rrs1* has been seen in previous GWAS studies, where a large linkage block was identified on chromosome 3H for seedling resistance in a diversity panel of spring barley (Hiddar et al., 2023) which was accompanied by QQ plots that showed a large deviation from the expected, and where there were two peaks in LD that spanned the centromeric region (Kunze et al., 2024).

Fine-mapping *Rrs1* to a 0.8 cM has identified ten candidate genes, however the *Rrs1* allele is in a centromeric region with high linkage disequilibrium and is not present in the reference Morex genome (Looseley et al., 2020). Further association analysis derived three markers near a protein kinase gene, indicating the *Rrs1* may be an allelic a member of the protein kinase gene family (Looseley et al., 2020). Examination of the mode of action of the *Rrs1* gene upon infection reveals that the resistance is incomplete, but that hyphal development is restricted, random in the direction of growth, and exhibits a delay in the collapse of the epidermal layer (Thirugnanasambandam et al., 2011). Additionally, marker trait associations on chromosome 3H have been found to contribute ~27 to 30% of the phenotypic variation for scald (Kunze et al., 2024; Noe et al., 2025), similar to the 27% phenotypic variation explained at *Rrs1* in this study. Importantly, additional SNP marker trait associations were found across the genome, including one that co-localized with *Rrs4* on chromosome 3H, and regions on chromosomes 2H, 4H, and 7H that can add to durable long term resistance.

637 ## 4.3 Agronomic traits can reduce disease infection

638 *Rhynchosporium graminicola* is a slow growing pathogen, requiring a three-week incubation period
639 between infection and lesion development. It capitalizes on the long early cold days of spring to
640 increase in spore load and infection. Agronomic variables can influence the rate of upward dispersal of
641 spores in the plant canopy. Winter survival is an important trait in crop improvement in northern
642 environments. The positive correlation between reduced plant density from poor winter survival (and
643 resulting reduced plot canopy) and reduced disease is an indicator of a microclimate and putative
644 reduced *R. graminicola* growth and/or spore load that leads to less disease. While not useful for
645 breeding purposes regarding management of scald through reduced canopy density, it is important to
646 include in GWAS models as a covariate for the phenotypic trait to improve SNP association identification.

647 Additional agronomic traits can help reduce infection. The negative correlation between heading date
648 and scald is indicative of an escape or avoidance mechanism, limiting the ability of *R. graminicola* conidia
649 to reach the upper leaves and spikes. The negative correlation between plant height and diseased leaf
650 area for scald also suggests an avoidance mechanism in plant defense, where elongative growth of plants
651 may outpace pathogen reproductive cycles thus delaying the rain splash dispersal of conidia to upper
652 leaves and glumes. The *sdw1* gene has previously been identified in GWAS for resistance to scald
653 (Loosely et al., 2018). In this study we identified a region on the short arm of chromosome 2H that
654 contributed to plant height and heading date (via *Ppd-H1*). The SNP association in this region may
655 contribute to either plant architectural traits, and/or active resistance, however it provides a target for
656 selection. With a rapidly mutating pathogen, breeding for earlier heading date and taller plants would
657 help provide additional mechanisms for plant defense. The implications for disease management as
658 shorter plants are often selected or desired for reduced lodging should include selection for resistance to
659 scald.

660 ## 4.4 When your population is not that diverse: Selection of GWAS model for adapted
661 multiparent populations

662 GWAS is a powerful tool for discovery of trait genetic architecture within a population. The
663 identification of SNP marker trait associations can also aid in confirmation of previously identified
664 genetic elements, if the allele is segregating in the population at the appropriate frequency and
665 amplitude to be detected. Understanding the allele effect, or percent variation explained by the
666 SNP/marker trait association can have implications that are important to move forward with more basic
667 genetic studies, or in selection for breeding programs. Most GWAS studies utilize diverse genetic
668 populations for the pursuit of trait association analysis, relying on the thousands of meiotic
669 recombination events between the diverse lines to determine the precise genetic location of marker trait
670 associations. The availability of high-density genotyping platforms for breeding programs offers the
671 ability to use GWAS for crop improvement (Spindel et al., 2013). Breeding programs often cycle many
672 semi-related genetic materials through preliminary breeding trials to select a set number of lines to
673 move forward for selection. While early generation selection of specifically targeted and agronomically
674 important high heritability traits may limit the germplasm pool, the preliminary breeding trials are often
675 replicated across locations. Harnessing the power of GWAS in large breeding populations can be very
676 useful for understanding the genetic architecture of segregating traits in breeding programs

677 The multiparent population was derived from a series of biparental crosses and presented a challenge in
678 how to separate population structure from effect. In this study, the SNP associations near *Rrs1* on
679 chromosome 3H varied from 174 Mb accounted for 19.4% in MLMMPVE), whereas the SNP association
680 at 442Mb accounted for 0.1% (MLM), 27.1% (FarmCPU) and 7.6% (BLINK). The FarmCPU model
681 appeared to be the least likely to overfit or overamplify type 1 associations in the structured population.
682 The MLM and MLMM GWAS models include both kinship and population structure whereas FarmCPU
683 includes kinship of associated markers and BLINK includes neither in their respective models. Population
684 structure and kinship are useful tools to reduce the confounding effects and to target unbiased marker
685 trait associations in large diverse populations. FarmCPU detected the largest amount of variation for
686 resistance to scald at the *Rrs1* locus on chromosome 3H, using more limited kinship but not population
687 structure.

688 Breeding for durable resistance to *R. graminicola* should encompass pyramiding a variety of mechanisms
689 to reduce the loss of yield and quality to scald. Major genes, such as *Rrs1*, provide a high level of
690 resistance and can be combined with QTLs and additional major resistance genes, especially those with
691 differing modes of action, to increase the resistance profile and decrease scald. In addition, selection for
692 agronomic traits, such as early flowering time and increased plant height can aid in limiting the vertical
693 spread of disease in the canopy and spike, in order to limit loss of quality and yield to scald.

694 **ACKNOWLEDGEMENTS**

695 The authors thank the field staff at the Cornell University Love Lab and Research Farm, and the small
696 grains field manager and crew, including David Benscher, Jason Schiller, Priscilla Thompson and James
697 Tanaka. We also thank Drs. Tyr Wieser-Hanks and Zhiwu Zhang for technical and theoretical help with
698 GAPIT version 3/FarmCPU, respectively. This work was supported by the USDA Barley Pest Initiative,
699 Hatch Project 149-950 and the New York State Department of Agriculture and Markets.

700 **CONFLICT OF INTEREST**

701 The authors declare no conflict of interest

702 **AUTHOR CONTRIBUTIONS**

703 Judith M. Kolkman: Conceptualization; Data curation; Formal analysis; Investigation; Methodology;
704 Visualization; Writing – original draft; Writing – review & editing.
705 Siim. S. Sepp: Investigation; Writing – review & editing.
706 Karl Kunze: Conceptualization; Investigation; Writing – review & editing.
707 Gary C. Bergstrom: Conceptualization; Funding acquisition; Project administration; Supervision; Writing –
708 review & editing.
709 Mark E. Sorrells: Conceptualization; Funding acquisition; Project administration; Supervision; Writing –
710 review & editing.

711 **ORCID**

712 Judith M. Kolkman: https://orcid.org/0000-0001-7388-7245
713 Siim S. Sepp: https://orcid.org/0000-0003-1181-7924
714 Karl H. Kunze: https://orcid.org/0000-0003-4548-1808
715 Gary Bergstrom: https://orcid.org/0000-0001-9613-270X
716 Mark E. Sorrells: https://orcid.org/0000-0002-7367-2663

SUPPLEMENTAL MATERIAL

DATA AVAILABILITY

Phenotypic data and GWAS results are available in supplemental tables; genotypic SNP dataset is available at (https://ics.hutton.ac.uk/50k)

REFERENCES

Ababa, G., Hailu, W., Shiferaw, T., Fekadu, W., & Alamerew, S. (2024). Adult-plant resistance to leaf scald and net form net blotch in food barley genotypes at a hot spot location in Ethiopia. *Heliyon*, *10*. https://doi.org/10.1016/j.heliyon.2024.e40529

Ababa, G., Kesho, A., Tadesse, Y., & Amare, D. (2023). Reviews of taxonomy, epidemiology, and management practices of the barley scald (*Rhynchosporium graminicola*) disease. *Heliyon*, *9*. https://doi.org/10.1016/j.heliyon.2023.e14315

Avrova, A., & Knogge, W. (2012). Rhynchosporium commune: A persistent threat to barley cultivation. *Molecular Plant Pathology*, *13*, 986–997. https://doi.org/10.1111/j.1364-3703.2012.00811.x

Ayesu-Offei, E. N., & Clare, B. G. (1970). Processes in the infection of barley leaves by *Rhynchosporium secalis*. *Australian Journal of Biological Sciences*, *23*(2), 300-308.

Bayer, M.M., Rapazote-Flores, P., Ganal, M., Hedley, P.E., Macaulay, M., Plieske, J., Ramsay, L., Russell, J., Shaw, P.D., Thomas, W., & Waugh, R. (2017). Development and evaluation of a barley 50k iSelect SNP array. *Frontiers in Plant Science*, *8*. https://doi.org/10.3389/fpls.2017.01792

Beigi, S., Zamanizadeh[1], H., Razavi, M., & Zare[2], R. (2013). Genetic diversity of Iranian isolates of barley scald pathogen (*Rhynchosporium secalis*) making use of molecular markers. *J. Agr. Sci. Tech. Vol. 15,* 843-854.

Bjørnstad, Å., Patil, V., Tekauz, A., Marøy, A.G., Skinnes, H., Jensen, A., Magnus, H., & Mackey, J. (2002). Genetics and resistance to scald (*Rhynchosporium secalis*) in barley (*Hordeum vulgare*) studied by near-isogenic lines: I. Markers and differential isolates. *Phytopathology*, *92*(7), 710-720.

Blachez, A.F., B.G.C., B.D., S.M.E. (2018). Evaluation of Fusarium head blight and foliar diseases on winter malting barley varieties in New York, 2017. *Plant Disease Management Reports 12*, CF028.

Bonferroni, C.E. (1936) Teoria statistica delle classi e calcolo delle probabilità, Pubblicazioni del R Istituto Superiore di Scienze Economiche e Commerciali di Firenze.

Box, G.E.P., & Cox, D.R. (1964). An Analysis of Transformations. *Journal of the Royal Statistical Society Series B: Statistical Methodology*, *26*, 211–243. https://doi.org/10.1111/j.2517-6161.1964.tb00553.x

Bradbury, P.J., Zhang, Z., Kroon, D.E., Casstevens, T.M., Ramdoss, Y., & Buckler, E.S. (2007). TASSEL: Software for association mapping of complex traits in diverse samples. *Bioinformatics*, *23*, 2633–2635. https://doi.org/10.1093/bioinformatics/btm308

Brunner, P.C., Schürch, S., & Mcdonald, B.A. (2007). The origin and colonization history of the barley scald pathogen *Rhynchosporium secalis*. *Journal of Evolutionary Biology*, *20*, 1311–1321. https://doi.org/10.1111/j.1420-9101.2007.01347.x

Burhenne, K., Kristensen, B.K., & Rasmussen, S.K. (2003). A new class of N-hydroxycinnamoyltransferases: Purification, cloning, and expression of a barley agmatine coumaroyltransferase (EC 2.3.1.64). *Journal of Biological Chemistry*, *278*, 13919–13927. https://doi.org/10.1074/jbc.M213041200

Büttner, B., Draba, V., Pillen, K., Schweizer, G., & Maurer, A. (2020). Identification of QTLs conferring resistance to scald (*Rhynchosporium commune*) in the barley nested association mapping population HEB-25. *BMC Genomics*, *21*. https://doi.org/10.1186/s12864-020-07258-7

Clare, S.J., Çelik Oğuz, A., Effertz, K., Karakaya, A., Azamparsa, M.R., & Brueggeman, R.S. (2023). Wild barley (*Hordeum spontaneum*) and landraces (*Hordeum vulgare*) from Turkey contain an abundance of novel *Rhynchosporium commune* resistance loci. *Theoretical and Applied Genetics*, *136*, 1–14. https://doi.org/10.1007/s00122-023-04245-w

Coulter, M., Büttner, B., Hofmann, K., Bayer, M., Ramsay, L., Schweizer, G., Waugh, R., Looseley, M.E., & Avrova, A. (2019). Characterisation of barley resistance to *Rhynchosporium* on chromosome 6HS. *Theoretical and Applied Genetics*, *132*, 1089–1107. https://doi.org/10.1007/s00122-018-3262-8

Crous, P.W., Braun, U., McDonald, B.A., Lennox, C.L., Edwards, J., Mann, R.C., Zaveri, A., Linde, C.C., Dyer, P.S., & Groenewald, J.Z. (2021). Redefining genera of cereal pathogens: *Oculimacula*, *Rhynchosporium* and *Spermospora*. *Fungal Systematics and Evolution*, *7*, 67–98. https://doi.org/10.3114/fuse.2021.07.04

Daba, S.D., Horsley, R., Brueggeman, R., Chao, S., & Mohammadi, M. (2019). Genome-wide association studies and candidate gene identification for leaf scald and net blotch in barley (*Hordeum vulgare* L.). *Plant Disease*, *103*, 880–889. https://doi.org/10.1094/PDIS-07-18-1190-RE

Davis, J. J. (1919). Notes on parasitic fungi in Wisconsin. VI. *Trans. Wis. Acad. Sci. Arts. Lett*, *19*, 705-727.

Doyle, J. J., & Doyle, J. L. (1987). A rapid procedure for DNA purification from small quantities of fresh leaf tissue. *Phytochemical bulletin*, *19*, 11-15.

Eckstein, P.E., Griffith, L.J., Zhang, X.M., Turkington, T.K., Colin, M.G., Holden, S., Walkowiak, S., Brar, G.S., & Beattie, A.D. (2024). An island of receptor-like genes at the *Rrs13* locus on barley chromosome 6HS co-locate with three novel sources of scald resistance. *Theoretical and Applied Genetics*, *137*, 249. https://doi.org/10.1007/s00122-024-04746-2

Flint-Garcia, S.A., Thuillet, A.C., Yu, J., Pressoir, G., Romero, S.M., Mitchell, S.E., Doebley, J., Kresovich, S., Goodman, M.M., & Buckler, E.S. (2005). Maize association population: A high-resolution platform for quantitative trait locus dissection. *Plant Journal*, *44*, 1054–1064. https://doi.org/10.1111/j.1365-313X.2005.02591.x

Frank, A. B. (1897). Über die Zerstörung der Gerste durch einen neuen Getreidepilz. *Wochenschr Brau*, *42*, 518-20.

Genger, R. K., Brown, A. H., Knogge, W., Nesbitt, K., & Burdon, J. J. (2003). Development of SCAR markers linked to a scald resistance gene derived from wild barley. *Euphytica*, *134*(2), 149-159.

Hautsalo, J., Novakazi, F., Jalli, M., Göransson, M., Manninen, O., Isolahti, M., Reitan, L., Bergersen, S., Krusell, L., Damsgård Robertsen, C., Orabi, J., Due Jensen, J., Jahoor, A., Bengtsson, T., Veteläinen, M., Alsheikh, M., Jansen, C., Windju, S., Vangdorf, N., Jensen, J.D., Hjortshøj, R.L., Robertsen, C.D., Bengtsson, T., Åhman, I., Hilmarsson, H.S., & Sveinsson, S. (2021). Pyramiding of scald resistance genes in four spring barley MAGIC populations. *Theoretical and Applied Genetics*, *134*, 3829–3843. https://doi.org/10.1007/s00122-021-03930-y

Hayes, P., Carrijo, D.R., Filichkin, T., Fisk, S., Helgerson, L., Hernandez, J., Meints, B., & Sorrells, M.E. (2021). Registration of 'Lightning' barley. *Journal of Plant Registrations*, *15*, 407–414. https://doi.org/10.1002/plr2.20129

Hiddar, H., Rehman, S., Belkadi, B., Filali-Maltouf, A., Al-Jaboobi, M., Verma, R.P.S., Gyawali, S., Kehel, Z., & Amri, A. (2023). Identification of sources of resistance to scald (*Rhynchosporium commune*) and of related genomic regions using genome-wide association in a mapping panel of spring barley. *Frontiers in Plant Science*, *14*. https://doi.org/10.3389/fpls.2023.1133404

Huang, M., Liu, X., Zhou, Y., Summers, R.M., & Zhang, Z. (2019). BLINK: A package for the next level of genome-wide association studies with both individuals and markers in the millions. *GigaScience*, *8*. https://doi.org/10.1093/gigascience/giy154

Ijaz, U., Zhao, C., Shahbala, S., & Zhou, M. (2024). Genome-wide association study for identification of marker-trait associations conferring resistance to scald from globally collected barley germplasm. *Phytopathology*, *114*, 1637–1645. https://doi.org/10.1094/PHYTO-01-24-0043-R

Kelly, J. D., Kolkman, J. M., & Schneider, K. (1998). Breeding for yield in dry bean (*Phaseolus vulgaris* L.). *Euphytica*, *102*(3), 343-356.

Kolkman, J.M., Bergrstom, G.C., Benscher, D., & Sorrells, M.E. (2025)(a). Reaction of winter malting barley cultivars and breeding lines to foliar diseases in New York, 2024. *Plant Health Progress*, *26*, 404–404. https://doi.org/10.1094/PHP-12-24-0172-PDMR

Kolkman, J.M., Bergrstom, G.C., Benscher, D., & Sorrells, M.E. (2025)(b). Reaction of spring malting barley cultivars and breeding lines to foliar diseases in New York, 2024. *Plant Health Progress*, *26*, 405–405. https://doi.org/10.1094/PHP-12-24-0173-PDMR

Kunze, K.H., Meints, B., Massman, C., Gutiérrez, L., Hayes, P.M., Smith, K.P., Bergstrom, G.C., & Sorrells, M.E. (2024). Genome-wide association of an organic naked barley diversity panel identified quantitative trait loci for disease resistance. *Plant Genome*, *17*(4), e20530. https://doi.org/10.1002/tpg2.20530

Lehnackers, H., & Knogge, W. (1990). Cytological studies on the infection of barley cultivars with known resistance genotypes by *Rhynchosporium secalis*. *Canadian Journal of Botany*, *68*(9), 1953-1961.

Linsell, K.J., Keiper, F.J., Forgan, A., & Oldach, K.H. (2011). New insights into the infection process of *Rhynchosporium secalis* in barley using GFP. *Fungal Genetics and Biology*, *48*, 124–131. https://doi.org/10.1016/j.fgb.2010.10.001

Liu, X., Huang, M., Fan, B., Buckler, E.S., & Zhang, Z. (2016). Iterative usage of fixed and random effect models for powerful and efficient genome-wide association studies. *PLoS Genetics*, *12*. https://doi.org/10.1371/journal.pgen.1005767

Looseley, M.E., Griffe, L.L., Büttner, B., Wright, K.M., Middlefell-Williams, J., Bull, H., Shaw, P.D., Macaulay, M., Booth, A., Schweizer, G., Russell, J.R., Waugh, R., Thomas, W.T.B., & Avrova, A. (2018). Resistance to *Rhynchosporium commune* in a collection of European spring barley germplasm. *Theoretical and Applied Genetics*, *131*, 2513–2528. https://doi.org/10.1007/s00122-018-3168-5

Looseley, M.E., Ramsay, L., Bull, H., Swanston, J.S., Shaw, P.D., Macaulay, M., Booth, A., Russell, J.R., Waugh, R., & Thomas, W.T.B. (2020). Association mapping of malting quality traits in UK spring and winter barley cultivar collections. *Theoretical and Applied Genetics*, *133*, 2567–2582. https://doi.org/10.1007/s00122-020-03618-9

Marzin, S., Hanemann, A., Sharma, S., Hensel, G., Kumlehn, J., Schweizer, G., & Röder, M.S. (2016). Are pectin esterase inhibitor genes involved in mediating resistance to *Rhynchosporium* commune in barley?. *PLoS ONE*, *11*(3), e0150485. https://doi.org/10.1371/journal.pone.0150485

Mascher, M., Gundlach, H., Himmelbach, A., Beier, S., Twardziok, S.O., Wicker, T., Radchuk, V., Dockter, C., Hedley, P.E., Russell, J., Bayer, M., Ramsay, L., Liu, H., Haberer, G., Zhang, X.Q., Zhang, Q., Barrero, R.A., Li, L., Taudien, S., Groth, M., Felder, M., Hastie, A., Šimková, H., Stanková, H., Vrána, J., Chan, S., Munõz-Amatriaín, M., Ounit, R., Wanamaker, S., Bolser, D., Colmsee, C., Schmutzer, T., Aliyeva-Schnorr, L., Grasso, S., Tanskanen, J., Chailyan, A., Sampath, D., Heavens, D., Clissold, L., Cao, S., Chapman, B., Dai, F., Han, Y., Li, H., Li, X., Lin, C., McCooke, J.K., Tan, C., Wang, P., Wang, S., Yin, S., Zhou, G., Poland, J.A., Bellgard, M.I., Borisjuk, L., Houben, A., Doleael, J., Ayling, S., Lonardi, S., Kersey, P., Langridge, P., Muehlbauer, G.J., Clark, M.D., Caccamo, M., Schulman, A.H., Mayer, K.F.X., Platzer, M., Close, T.J., Scholz, U., Hansson, M., Zhang, G., Braumann, I., Spannagl, M., Li, C., Waugh, R., & Stein, N. (2017). A chromosome

conformation capture ordered sequence of the barley genome. *Nature*, *544*, 427–433. https://doi.org/10.1038/nature22043

Mascher, M., Wicker, T., Jenkins, J., Plott, C., Lux, T., Koh, C.S., Ens, J., Gundlach, H., Boston, L.B., Tulpová, Z., Holden, S., Hernández-Pinzón, I., Scholz, U., Mayer, K.F.X., Spannagl, M., Pozniak, C.J., Sharpe, A.G., Simková, H., Moscou, M.J., Grimwood, J., Schmutz, J., & Stein, N. (2021). Long-read sequence assembly: A technical evaluation in barley. *Plant Cell*, *33*, 1888–1906. https://doi.org/10.1093/plcell/koab077

Mcdonald, B.A. (2015). How can research on pathogen population biology suggest disease management strategies? The example of barley scald (*Rhynchosporium commune*). *Plant Pathology*, *64*, 1005–1013. https://doi.org/10.1111/ppa.12415

Noe, S.M., Åstrand, J., Zakieh, M., Singh, P.K., Johansson, E., & Chawade, A. (2025). Harnessing novel genetic markers for scald resistance from gene bank spring barley genotypes. *BMC Plant Biology*, *25*(1), 781. https://doi.org/10.1186/s12870-025-06813-2

Patil, V., Bjørnstad, Å., & Mackey, J. (2003). Molecular mapping of a new gene Rrs4 CI 11549 for resistance to barley scald (*Rhynchosporium secalis*). *Molecular Breeding*, *12*(2), 169-183.

Ryan, C.C., & Grivell, C.J. (1974). An Electron Microscope Study of the Outer Layers of Barley Leaves Infected with *Rhynchosporium secalis*. *Aust. J. Plant Physiol*

Segura, V., Vilhjálmsson, B.J., Platt, A., Korte, A., Seren, Ü., Long, Q., & Nordborg, M. (2012). An efficient multi-locus mixed-model approach for genome-wide association studies in structured populations. *Nature Genetics*, *44*, 825–830. https://doi.org/10.1038/ng.2314

Shipton, W. A., Boyd, W. J. R., & Ali, S. M. (1974). Scald of barley. 839-861.

Shrestha, R.K., & Lindsey, L.E. (2019). Agronomic management of malting barley and research needs to meet demand by the craft brew industry. *Agronomy Journal*, *111*, 1570–1580. https://doi.org/10.2134/agronj2018.12.0787

Siller, A., Hashemi, M., Wise, C., Smychkovich, A., & Darby, H. (2021). Date of planting and nitrogen management for winter malt barley production in the northeast, USA. *Agronomy*, *11*. https://doi.org/10.3390/AGRONOMY11040797

Spindel, J., Wright, M., Chen, C., Cobb, J., Gage, J., Harrington, S., Lorieux, M., Ahmadi, N., & McCouch, S. (2013). Bridging the genotyping gap: Using genotyping by sequencing (GBS) to add high-density SNP markers and new value to traditional bi-parental mapping and breeding populations. *Theoretical and Applied Genetics*, *126*, 2699–2716. https://doi.org/10.1007/s00122-013-2166-x

Thirugnanasambandam, A., Wright, K.M., Atkins, S.D., Whisson, S.C., & Newton, A.C. (2011). Infection of *Rrs1* barley by an incompatible race of the fungus *Rhynchosporium secalis* expressing the green fluorescent protein. *Plant Pathology*, *60*, 513–521. https://doi.org/10.1111/j.1365-3059.2010.02393.x

Tibbs Cortes, L., Zhang, Z., & Yu, J. (2021). Status and prospects of genome-wide association studies in plants. *Plant Genome*, *14*(1), e20077. https://doi.org/10.1002/tpg2.20077

Turner, A., Beales, J., Faure, S., Dunford, R. P., & Laurie, D. A. (2005). The pseudo-response regulator *Ppd-H1* provides adaptation to photoperiod in barley. *Science*, *310*(5750), 1031-1034.

Wagner, C., Schweizer, G., Krämer, M., Dehmer-Badani, A.G., Ordon, F., & Friedt, W. (2008). The complex quantitative barley-*Rhynchosporium secalis* interaction: Newly identified QTL may represent already known resistance genes. *Theoretical and Applied Genetics*, *118*, 113–122. https://doi.org/10.1007/s00122-008-0881-5

Wang, J., & Zhang, Z. (2021). GAPIT Version 3: Boosting Power and Accuracy for Genomic Association and Prediction. *Genomics, Proteomics and Bioinformatics*, *19*, 629–640. https://doi.org/10.1016/j.gpb.2021.08.005

Wang, Y., Xu, Y., Gupta, S., Zhou, Y., Wallwork, H., Zhou, G., Broughton, S., Zhang, X.Q., Tan, C., Westcott, S., Moody, D., Sun, D., Loughman, R., Zhang, W., & Li, C. (2020). Fine mapping QSc.VR4, an effective and stable scald resistance locus in barley (*Hordeum vulgare* L.), to a 0.38-Mb region enriched with LRR-RLK and GLP genes. *Theoretical and Applied Genetics*, *133*, 2307–2321. https://doi.org/10.1007/s00122-020-03599-9

Xu, Y., Jia, Q., Zhou, G., Zhang, X.Q., Angessa, T., Broughton, S., Yan, G., Zhang, W., & Li, C. (2017). Characterization of the *sdw1* semi-dwarf gene in barley. *BMC Plant Biology*, *17*. https://doi.org/10.1186/s12870-016-0964-4

Yu, J., Pressoir, G., Briggs, W.H., Bi, I.V., Yamasaki, M., Doebley, J.F., Mcmullen, M.D., Gaut, B.S., Nielsen, D.M., Holland, J.B., Kresovich, S., & Buckler, E.S. (2006). A unified mixed-model method for association mapping that accounts for multiple levels of relatedness *38*, 203–208. https://doi.org/10.1038/ng1702

Zaffarano, P.L., McDonald, B.A., & Linde, C.C. (2008). Rapid speciation following recent host shifts in the plant pathogenic fungus *Rhynchosporium*. *Evolution*, *62*, 1418–1436. https://doi.org/10.1111/j.1558-5646.2008.00390.x

Zaffarano, P.L., McDonald, B.A., & Linde, C.C. (2011). Two new species of *Rhynchosporium*. *Mycologia*, *103*, 195–202. https://doi.org/10.3852/10-119

Zhang, X., Ovenden, B., & Milgate, A. (2020). Recent insights into barley and *Rhynchosporium commune* interactions. *Molecular Plant Pathology*, *21*, 1111–1128. https://doi.org/10.1111/mpp.12945

Zhang, Z., Ersoz, E., Lai, C.Q., Todhunter, R.J., Tiwari, H.K., Gore, M.A., Bradbury, P.J., Yu, J., Arnett, D.K., Ordovas, J.M., & Buckler, E.S. (2010). Mixed linear model approach adapted for genome-wide association studies. *Nature Genetics*, *42*, 355–360. https://doi.org/10.1038/ng.546

938

939 **Supplemental figures**

940

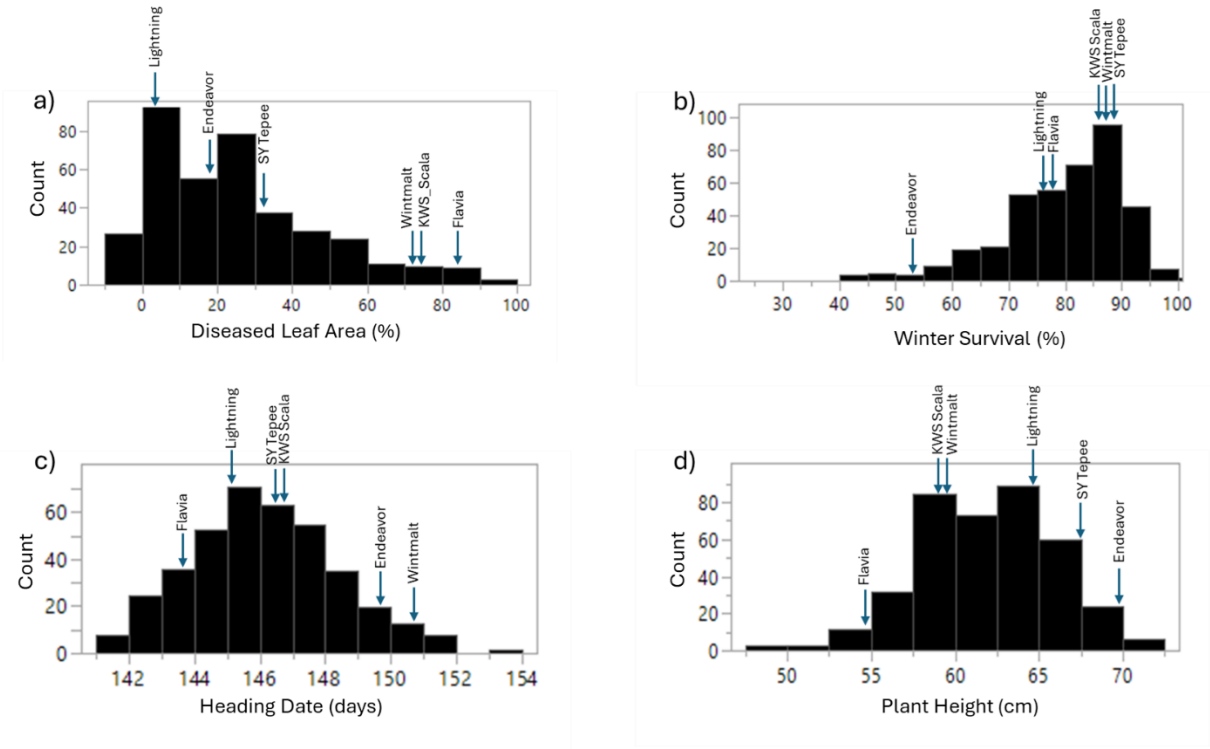

941

942 Figure S1. Frequency distribution for a) scald diseased leaf area, b) winter survival, c) heading date
943 (Julian), and d) plant height shows transgressive segregation in the population of 377 lines derived from
944 the parental lines. Values for each parental line are indicated by the blue arrows for each of the disease
945 and agronomic traits. 'Endeavor', a check cultivar grown across blocks and experiments is also shown for
946 comparison.

947

948

949

950

951

952

953

954

955

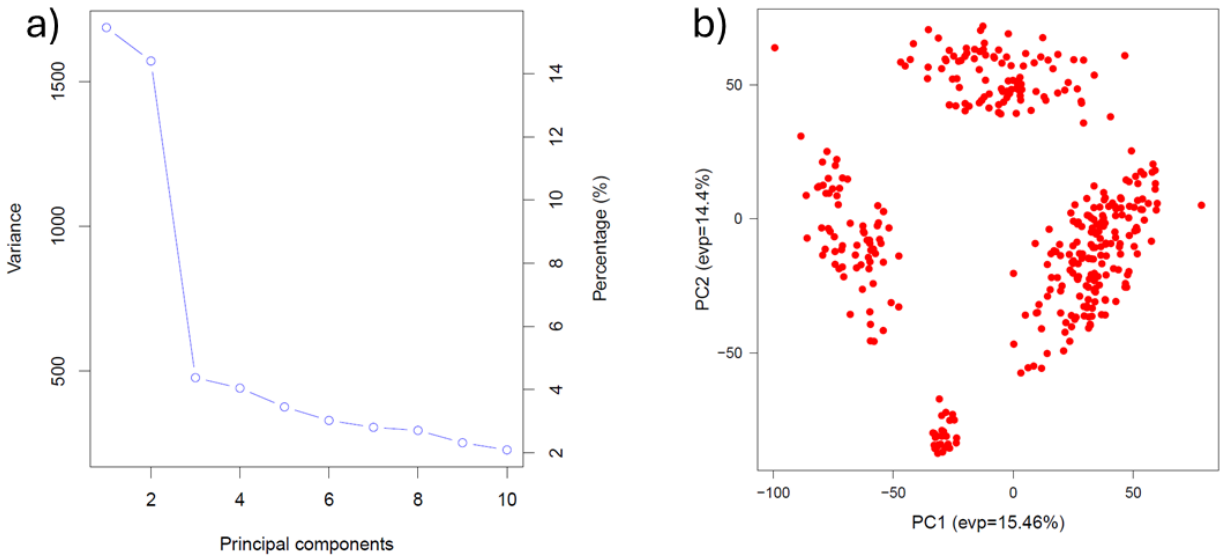

Figure S2. Principal component analysis for the 374 lines of the multiparent population displaying a) PCA eigenvalues and b) genotype clustering for PCA = 2, indicating clustering into 4 subgroups.

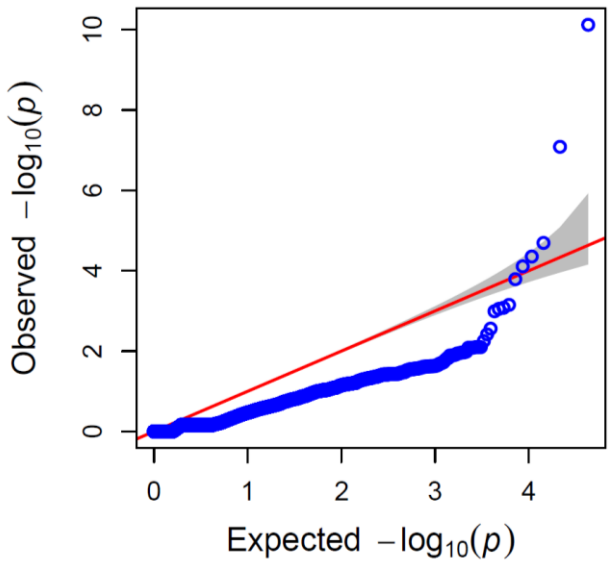

Figure S3. Quantile-quantile plot for FarmCPU GWAS model for resistance to scald in winter malting barley using PCA=2 as a covariate.

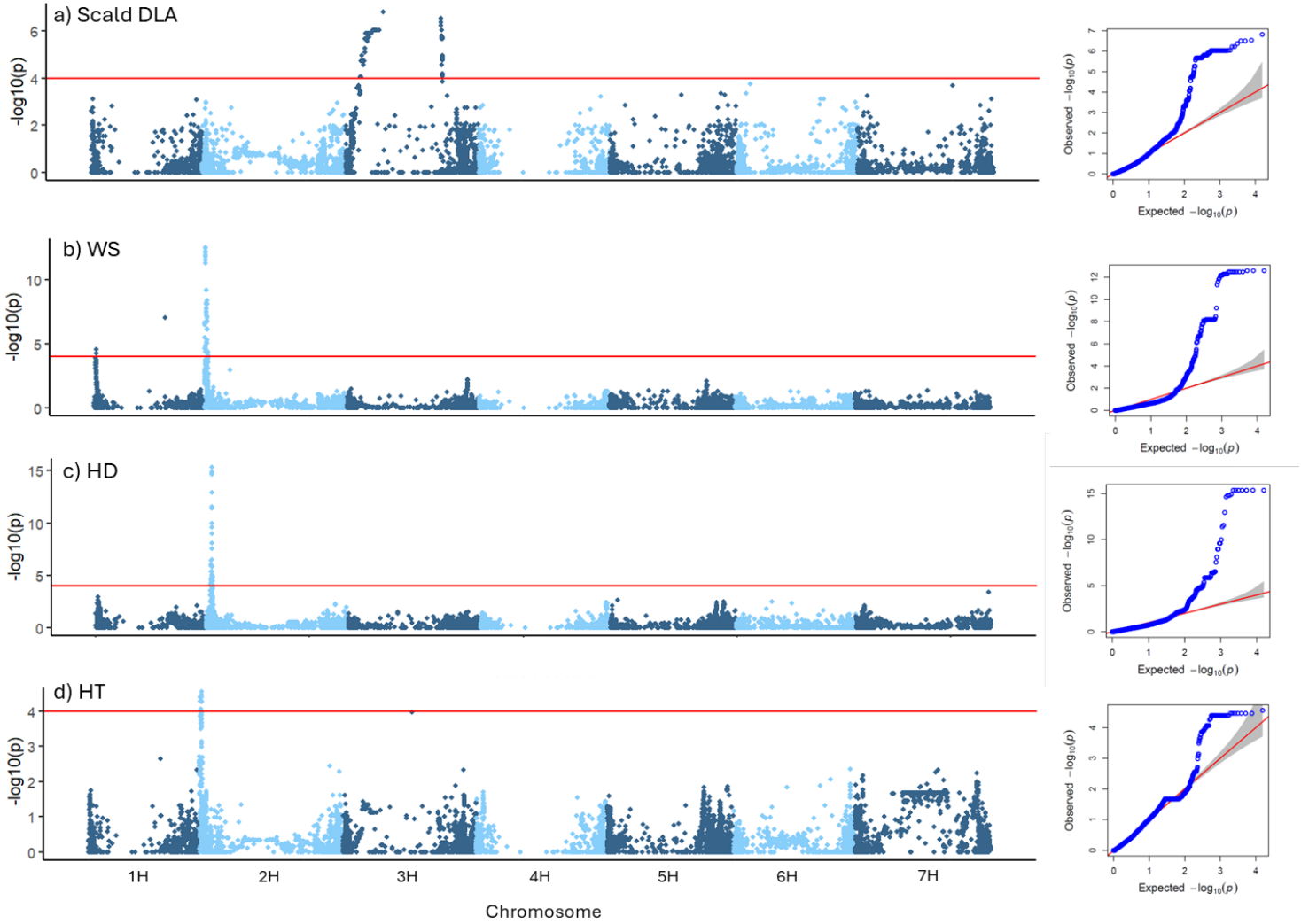

Figure S4: Manhattan plots for a) resistance to scald (DLA), b) winter survival (WS), c) heading date (HD), and d) plant height (HT) using the 374 lines and 15,463 SNPs in the MLM GWAS mode, with corresponding QQ plots (right). DLA BLUPs for resistance to scald were calculated without using WS, HD date and HT as covariates in the BLUP model. All traits BLUPs were calculated in four environments across 2022 and 2023. The red horizontal line indicates the QQ plot – determined threshold of $-\log_{10}(p)$ of 4.0.

980 **Supplemental Tables**

981 Table S1. Diseased leaf area for scald, winter survival, heading date and plant height in the multiparent
982 population across four environments.

983 Table S2. Least square means of diseased leaf area for scald, winter survival, heading date and plant
984 height for the multiparent population across four environments.

985 Table S3. Transformed diseased leaf area BLUPs with and without agronomic covariates, as well as the
986 transformed winter survival, heading date and plant height across four environments.

987 Table S4. SNP association statistics for diseased leaf area for scald (with agronomic trait covariates) in the
988 multiparent population for the MLM, MLMM, FarmCPU and BLINK GWAS models.

989 Table S5. HVS3 SCAR marker allele sizes linked to *Rrs1* in the multiparent population.

990 Table S6. SNP association statistics for diseased leaf area for scald (without agronomic trait covariates),
991 winter survival, heading date and plant height in the multiparent population for MLM and FarmCPU
992 GWAS models.